2009

High temperature studies of thin film Aluminum Nitride and piezoelectric characterization of mesa structures

Richard Farrell
West Virginia University

High Temperature Studies of Thin Film Aluminum Nitride and Piezoelectric Characterization of Mesa Structures

Richard Farrell

Thesis submitted to the College of Engineering and Mineral Resources
at West Virginia University
in partial fulfillment of the requirements
for the degree of

Master of Science
in
Electrical Engineering

Dimitris Korakakis, Ph.D., Chair
Parviz Famouri, Ph.D.
Xian-An Cao, Ph.D.

Lane Department of Computer Science and Electrical Engineering

Morgantown, West Virginia
2009

Keywords: aluminum nitride, piezoelectric, high temperature

ABSTRACT

HIGH TEMPERATURE STUDIES OF THIN FILM ALUMINUM NITRIDE AND PIEZOELECTRIC CHARACTERIZATION OF MESA STRUCTURES

by Richard Farrell

Aluminum Nitride (AlN) is a group III-V compound that grows in a hexagonal wurtzite crystal structure and is a popular material for microelectromechanical systems (MEMS) due in part to its piezoelectricity, inertness and tolerance to high temperatures. High temperature stability is an essential characteristic for numerous MEMS applications, so one of the goals of this work is to determine how the material properties of AlN are affected by exposure to high temperatures and harsh environments. 3D AlN devices are also investigated to determine the effect of electric field isolation on the piezoelectric response of AlN.

A Rapid Thermal Annealing (RTA) system was used to anneal the AlN films at temperatures up to 1000°C in ambient and controlled environments. The oxygen content of films annealed in an ambient environment was measured along with the piezoelectric coefficient (d_{33}) to determine the effect of oxygen incorporation on the piezoelectric response of the films. A high temperature test chamber was designed and built for in-situ high temperature piezoelectric measurements of AlN. The results of the ex-situ and in-situ high temperature experiments, the effects of oxidation on the piezoelectric response of AlN, and methods used to protect the films from oxidation are discussed.

Typically, a metal layer covering the entire AlN film is used as a top electrode in d_{33} measurements. In this work, circular AlN mesa structures, consisting of an AlN layer, with thicknesses between 200-1000nm, between two ~200nm metal layers, have been created. By decreasing the contact size and limiting the surface area of the AlN film, clamping effects are reduced. This configuration also minimizes non-normal electric field lines between the top and bottom contacts and further isolates the d_{33} piezoelectric coefficient. The devices are constructed using two different fabrication methods and the piezoelectric and electrical properties have been studied.

ACKNOWLEDGMENTS

I would like to express my deepest gratitude to everyone who made this work possible.

First I would like to thank my family, who has provided me with love and support throughout this process. Without them, none of this would be possible. I would like to thank my research advisor, Dr. Korakakis, for his guidance, support, and patience throughout my undergraduate and graduate career. I would also like to thank the other members of my committee, Dr. Famouri and Dr. Cao, who have provided valuable technical guidance. I could not have completed this work without helpful discussions and input from the members of the research lab: Vincent Pagán, Adam Kabulski, John Harman, Kalyan Reddy Kasarla, Lee Rodak and all others who I may not have mentioned. Finally, I would like to thank Dr. Brown for the cleanroom training and technical assistance with the research equipment.

TABLE OF CONTENTS

LIST OF FIGURES

LIST OF TABLES

CHAPTER 1: ALUMINUM NITRIDE MEMS

1.1) Introduction to Microelectromechanical Systems

Microelectromechanical systems (MEMS) are micro-fabricated systems that contain both electrical and mechanical components and are traditionally characterized as sensors or actuators. Sensors generate an electrical signal from physical stimuli and actuators convert electrical energy into some form of controlled motion. Examples of MEMS sensors and actuators can be seen in a variety of applications. MEMS sensors are used for automobile airbag deployment control, intracardiac blood pressure monitoring, and chemical sensors while MEMS actuators are used for ink-dispensing nozzles in inkjet printers, valves and pumps in miniature fluidic systems, and in video display systems using micromirrors [1-4].

1.2) Introduction to the Piezoelectric Effect

Operation of MEMS devices relies on electrical to mechanical transduction converting a mechanical phenomenon into a measurable electrical quantity or vice versa. MEMS actuators are fabricated to convert an electrical signal into a measurable mechanical quantity through various methods of transduction. Common transduction methods include piezoresistivity, capacitance changes, magnetic fields, and piezoelectricity [4]. Throughout this research, piezoelectricity is the transduction method used to actuate MEMS devices.

Piezoelectricity is a physical phenomenon where an applied force generates an electrical charge on the surface of a material, with the amount of charge directly related to the applied force. The piezoelectric effect is exhibited in non-centrosymmetric crystal classes where the unit cell contains positive and negative ions that are not symmetrically oriented with respect to each other resulting in a net charge. In a material with symmetric charge, the positive and negative ions cancel and the net charge is zero. The stress caused by an applied force causes a slight change in the positively and negatively charged ions in the material creating electric dipole moments. A surface charge-induced electric field cancels the stress-induced electric field from the dipoles. The reverse is also true; application of an electric field across the material results in a compensatory deformation of that material [5-6]. The linear relationship between the mechanical force applied to the material and the charge induced makes this transduction method ideal for MEMS sensors and actuators.

The piezoelectric coefficient (d_{33}) is used to quantify the piezoelectric effect in the direction normal to the substrate (c-axis). The direct piezoelectric effect is measured by applying a force and measuring the resultant charge produced (units of pC/N). The indirect piezoelectric effect is measured by applying a voltage and measuring the picometer level displacement of the film by using a laser vibrometer or white light interferometer. The unit of measure for the indirect piezoelectric coefficient is pm/V.

The polarization of a piezoelectric film plays a large part in the piezoelectric response of non-ferroelectric materials. In a polycrystalline film, the electric dipoles may

be oriented at random so the material may exhibit little to no piezoelectric effect. By heating the material while applying a strong electric field, the polarization can be improved. The heat allows the molecules to move, while the strong electric field causes the dipoles to face in the same direction [7]. Random polarization in piezoelectric materials may result in a limited piezoelectric response, so it is important to produce high quality c-axis oriented materials to produce the largest response in piezoelectric MEMS devices. Optimization of deposition techniques such as reactive sputtering or epitaxial growth can ensure a net c-axis polarization in polycrystalline films.

Piezoelectric materials commonly used for MEMS applications are zinc oxide (ZnO), lead zirconate titanate (PZT), lithium niobate ($LiNbO_3$), and aluminum nitride (AlN). Despite exhibiting a lower d_{33} than the other materials, AlN is the focus of this study because it does not exhibit the same physical limitations as the other materials at high temperatures or in harsh environments [8]. This makes it an ideal material for high temperature MEMS applications.

1.3) Introduction to Aluminum Nitride

Aluminum nitride (AlN) is a III-V compound with a hexagonal wurtzite crystal structure that has gained increasing interest for piezoelectric and photoelectric applications. AlN has a high decomposition temperature and low electrical, but high thermal conductivity making it an ideal candidate for use in high temperature applications and in

harsh environments [9]. Its wide bandgap (6.2 eV), high refractive index (1.9 – 2.1), and compatibility with other III-nitrides makes AlN an ideal material for use in ultraviolet optoelectronic applications [10]. Interest has been generated in the development of surface acoustic wave (SAW) and bulk acoustic wave (BAW) devices using AlN because of its excellent piezoelectricity, high surface acoustic wave velocity, substantial electromechanical coupling coefficient, and high temperature stability [11-12].

There are many different methods for obtaining AlN layers such as reactive sputtering, chemical vapor deposition (CVD), vapor phase epitaxy or molecular beam epitaxy (MBE). Sputtering is a low cost, versatile, low temperature deposition technique that is widely used to obtain AlN material [13]. Sputtered AlN is typically polycrystalline which may exhibit a reduced piezoelectric response due to random crystal orientation; however chamber conditions, substrate material, and pre-deposition cleaning techniques may be adjusted to increase the response of the material. Performing a hydrofluoric (HF) acid dip on the Si substrate and pre-sputtering the Al target to clean and equilibrate the target surface prior to film deposition reduces the chance of film contamination [14]. Adjusting the nitrogen (N_2) concentration in the sputtering chamber and increasing the power density of the deposition produces a higher quality film so the piezoelectric response may be increased. Substrate material has also been reported to increase the piezoelectric response in AlN films due to different nucleation surfaces created by the different materials [15]. Studies have shown that the difference in the piezoelectric effect is closely related to the work function of the substrate and contact metal [16].

Metalorganic vapor phase epitaxy (MOVPE) is a high temperature growth technique which produces high quality c-axis oriented AlN. An MOVPE deposits III-V materials using a chemical reaction between a metalorganic material (such as trimethylaluminum) and a reactive gas (such as ammonia) at temperatures higher than 1300°C [17]. MOVPE-grown AlN films typically exhibit a larger piezoelectric coefficient and are more resistant to oxidation and material decomposition at high temperatures compared to sputtered AlN. MOVPE-AlN grown on GaN produces nearly crystalline material due to the small lattice mismatch between III-nitrides and will be discussed in this thesis.

This work investigates the room temperature piezoelectric response of AlN devices using different geometries and establishes a procedure for high temperature studies of the piezoelectric response of AlN films and devices. The effects of high temperature annealing on the oxidation and piezoelectric response of sputtered and MOVPE-grown AlN films are studied in depth along with the development and piezoelectric characterization of 3D AlN devices. A procedure for in-situ high temperature piezoelectric testing of AlN films has been established and will be used for high temperature testing of 3D AlN devices in subsequent work.

CHAPTER 2: HIGH TEMPERATURE ANNEALING STUDIES OF ALN FILMS

2.1) Motivation

Aluminum nitride (AlN) is an attractive material for the fabrication of microelectrocmechanical systems (MEMS) devices due in part to its piezoelectricity, inertness and tolerance to high temperatures. One of the main advantages of AlN film is that its piezoelectric properties are preserved after annealing at temperatures as high as 1200°C [18]. Other materials, such as lead zirconate titanate (PZT), exhibit a higher piezoelectric response than AlN, however those materials lose their properties after annealing above their Curie temperature. The piezoelectric response of PZT drastically and irreversibly decreases at temperatures as low as 250°C [19]. AlN has no known Curie point because the piezoelectric response in AlN originates from the oriented crystalline nature [20].

One of the main inhibiting factors in the piezoelectric response of AlN at high temperatures is the incorporation of oxygen which is detrimental to both the structural and piezoelectric properties in the film [21]. The amount of oxygen required to eliminate the piezoelectric response is under debate but some groups declare that AlN films could contain as high as 7% (atomic) oxygen and still exhibit a high piezoelectric response [22]. Protective measures taken prior to exposure at high temperatures in order to preserve the piezoelectric response of AlN films are discussed in this chapter.

2.2) Background

AlN is very useful in the electronics industry for its high thermal conductivity, good electrical insulation [23], and thermal expansion similar to silicon [24]. Oxidation of AlN films is useful for adhesion of deposited metal layers, but it also causes a decrease in the thermal conductivity and piezoelectricity of the film [25-26]. Therefore, the oxidation behavior of AlN is an important factor when considering electronics devices for use in high temperature environments. AlN powder annealed in ambient conditions begins to oxidize at 700°C. The material oxidizes at a linear rate below 1000°C and a parabolic rate above that temperature [27]. Above 1000°C, after an initial increase, the oxidation rate decreases slightly indicating that the surface is completely oxidized [28]. The atomic percentage of oxygen in AlN films is measured in this work using energy dispersive X-ray analysis (EDAX).

Since the Curie temperature of the material is known to be higher than 1200°C, the main inhibitor of the piezoelectric response of AlN devices at high temperature is oxidation and material decomposition. Many materials have been studied and used as a protective layer to preserve the properties of MEMS devices during exposure to harsh environments. Silicon nitride (Si_3N_4) is among many materials used for this application due to its high temperature stability, resistance to thermal shock and hardness [29]. Si_3N_4 is thermally stable in a nitrogen atmosphere up to 1880°C and in the absence of N_2, decomposition becomes significant at temperatures above 1200°C. In this work, ex-situ annealing tests

expose AlN to temperatures as high as 1000°C in an ambient environment and Si_3N_4 is tested as a protected layer to reduce surface oxidation and maintain the piezoelectric response of the film.

High temperature annealing can also be used to improve the quality of AlN films by improving the hardness and reducing the residual stress of the films, however there is debate over whether the piezoelectric response is improved as a direct result [30]. While annealing at high temperatures has reportedly improved the crystal quality of AlN, Vergara *et al* state the improvement in grain size and crystal orientation does not directly result in an increase of the piezoelectric coefficient. In their study, sputtered amorphous AlN films annealed at high temperatures did not experience a significant change in crystal quality while AlN films with a clear c-axis orientation improved as verified by the X-ray diffraction (XRD) rocking curve. The improvements in polycrystalline films did not result in a significant increase in piezoelectric response. Vergara *et al* claim the presence of grains with opposite piezoelectric polarity causes a reduction in the net piezoelectric polarity, leading to a poor response [31].

High temperature piezoelectric measurements of AlN films using laser Doppler vibrometry (LDV) are not widely reported. Kano *et al* used rf-sputtered 1200 nm thick AlN films to reveal that AlN can be used as an actuator with a constant output velocity up to 300°C [32]. They reported a constant vibration velocity at temperatures ranging from 20°C to 300°C which converted to a d_{33} value of 1.38 pC/N. Direct measurements of the piezoelectric response have been taken at temperatures as high as 700°C by Kishi *et al*.

This group applied a load pressure of 200 ± 40 N and recorded a constant output voltage up to 400°C but the voltage decreased rapidly up to 700°C. When measurements were taken again at room temperature, the film produced only 50% of the initial response [33]. The reduction in piezoelectric response was attributed to degradation of electrical probes. The results of in-situ high temperature piezoelectric measurements of sputtered and MOVPE-grown AlN films using laser Doppler vibrometry will be discussed in this chapter.

2.3) Ex-Situ Annealing Study

This study reports the effects of high temperature annealing on sputtered and metalorganic vapor phase epitaxy (MOVPE)-grown AlN thin films. The films were exposed to high temperatures ranging up to 1000°C and the post annealing characterization is reported. The relationship between temperature and surface oxidation was explored then the effects of oxidation on the piezoelectric coefficient were determined. Protecting AlN from oxidation is important for preservation of the piezoelectric response of the film at high temperatures so plasma enhanced chemical vapor deposition (PECVD)-deposited silicon nitride (Si_3N_4) was used as a thin protective capping layer and thermal cycling was also tested as a means of protecting the films.

Sputtered films were deposited at room temperature onto a 350 μm thick (1 0 0)-oriented *p*-type silicon substrate using a CVC 610 direct current (DC) magnetron sputtering system in an Ar/N_2 environment. Film thickness for the study ranged from 300 to 500 nm

and the sputtering parameters are outlined in Table 1. MOVPE-grown AlN was grown in an AIXTRON 200/4 RF-S horizontal reactor on 2 inch (1 0 0) *p*-type silicon substrates. The growth temperature was approximately 1100 °C and the reactor pressure was 50 mbar. Trimethylaluminum (TMAl) and ammonia (NH_3) were used as Al and N source precursors with flows of 12 μmol/min and 1.5 slm respectively. Hydrogen was used as the carrier gas.

Table 1: Sputtering conditions for AlN film deposition

Parameter	Value
Al Target (%)	99.999
Target Size	8" diameter
DC Power (W)	500
Substrate Temperature	Room Temperature
Sputtering Pressure (mTorr)	30
Sputtering time (minutes)	35
N_2 concentration (%)	99.999
Ar/N_2	3/27

The AlN thin films were annealed in an Annealsys AS-Micro rapid thermal annealing (RTA) furnace at temperatures ranging from room temperature to 1000°C for 5 minutes. The RTA chamber is not hermetically sealed and annealing was done in an ambient environment to allow the films to oxidize. The oxide thickness on the surface of the films and refractive index was measured using a J.A. Woollam M-2000 spectroscopic

ellipsometer. Figure 1 shows the oxide thickness on the surface of sputtered and MOVPE-grown AlN after annealing in an ambient environment.

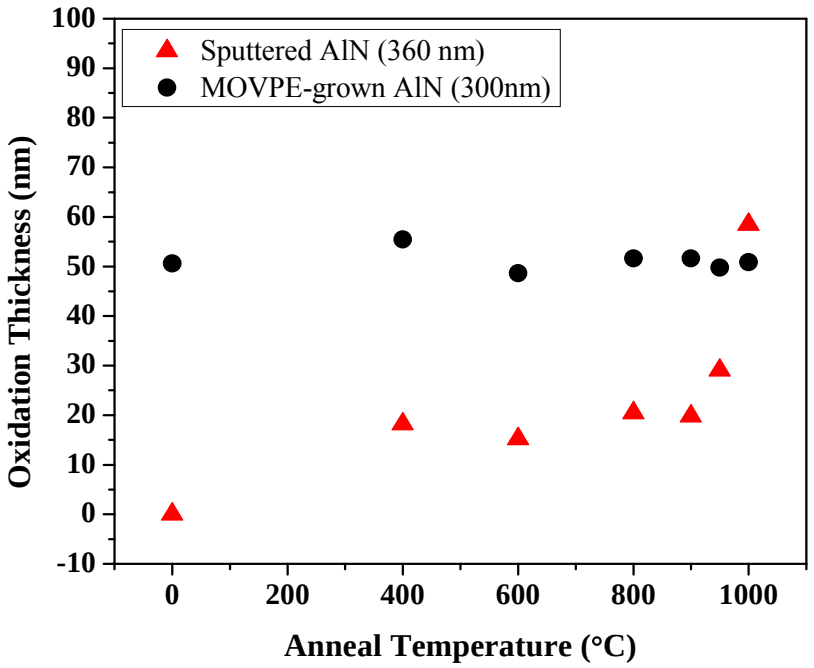

Figure 1 – Surface oxidation of sputtered and MOVPE-grown AlN films

The oxide thickness on the surface of sputtered films gradually increases with temperature up to 850°C, exponentially increasing above 900°C. Surface oxidation in MOVPE-grown films remains relatively constant from room temperature measurements up to 1000°C. AlN films grown in an MOVPE system terminate at the Al face, and due to the high quality of the film and crystal symmetry, the exposed surface is primarily Al-polar which causes uniform oxidation of the film when exposed to air. The uniform oxide layer formed on the surface protects the film from harsh environments as shown in Figure 1.

The atomic percentage of oxygen throughout these films is measured using energy dispersive X-ray analysis (EDAX). The EDAX results displaying the oxidation trends throughout sputtered and MOVPE-grown AlN films are shown in Figure 2.

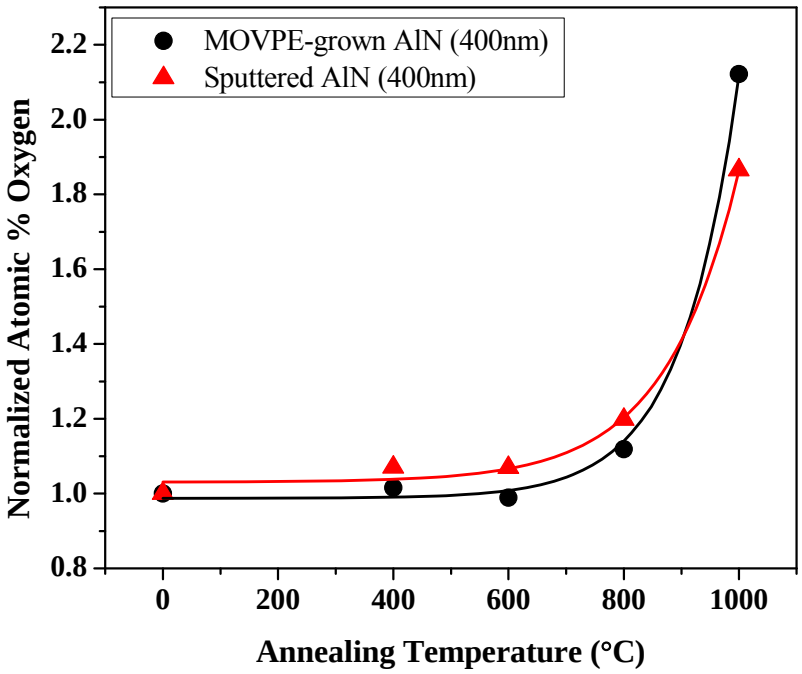

Figure 2 – Atomic % of oxygen in sputtered and MOVPE-grown AlN

The results in Figures 1 and 2 shows that sputtered films oxidize more than MOVPE-grown films at lower temperatures probably due to the different crystalline quality achieved by the two methods of deposition. At temperatures close to 1000°C both films oxidize rapidly as expected.

Solid circular platinum contacts were deposited on the top of the AlN films after annealing using a standard photolithography technique and an aluminum backside contact was sputtered onto the back of each wafer. An alternating current (AC) signal was used to

actuate the films and an MSV-100 scanning head laser Doppler vibrometer (LDV) was utilized to measure the picometer-level displacement of the AlN films in order to determine how the piezoelectric properties of thin AlN films respond after exposure to high temperatures. All piezoelectric measurements described in this section were taken at room temperature either prior to annealing or after RTA processing. In-situ high temperature piezoelectric measurements are discussed later in this chapter.

The piezoelectric coefficient (d_{33}) of annealed samples is lower compared to unannealed samples as shown in Table 2. After annealing at 1000°C, the measured d_{33} of both sputtered and MOVPE-grown films reduced to about 25% of the original response of the as-grown films. Oxidation results in Figures 1 and 2 and the d_{33} results in Table 2 lead to the conclusion that surface oxidation in AlN films drastically reduces piezoelectric response. These films were 300-400 nm thick.

Table 2 – Measured d_{33} of annealed and unannealed AlN films

Sample	d_{33} (pm/V)
Sputtered Unannealed	3.31
Sputtered Annealed (1000°C)	1.03
MOVPE-grown Unannealed	15.38
MOVPE-grown Annealed (1000°C)	4.08

Various methods of protection were sought to preserve the quality of the film and the piezoelectric response during annealing. One method of protection, called thermal cycling, protects the surface by annealing AlN to a temperature known to improve the crystal quality of the film (600°C) before the film is cooled and annealed at higher

temperatures [9]. As earlier results have shown, films of higher crystal quality are less susceptible to oxidation; therefore annealing the films to 600°C prior to annealing at higher temperatures should serve as a protective measure. Figure 3 shows the relationship of the oxide thickness of a cycled film and an as-deposited film as a function of annealing temperature.

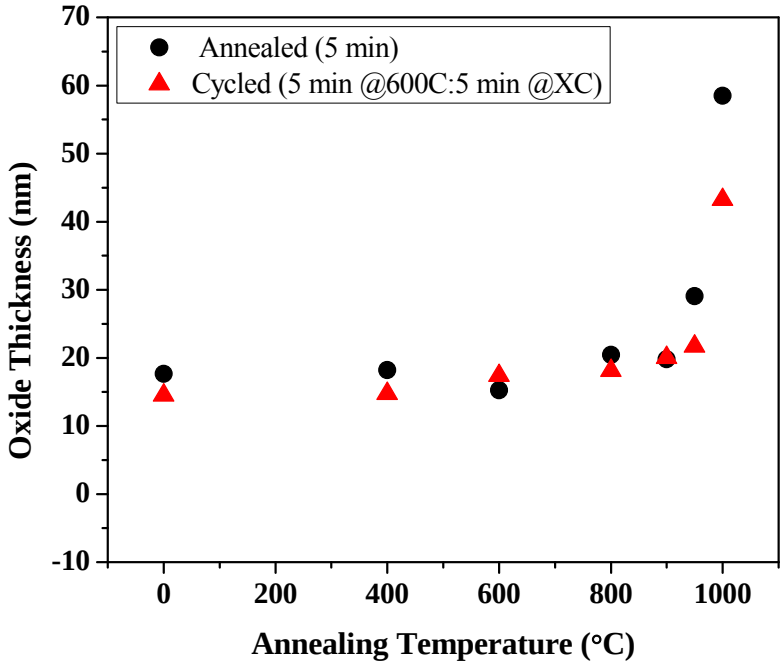

Figure 3 – Oxide thickness of cycled and as-grown sputtered AlN

The trends in Figure 3 indicate that cycling has little effect on the oxide thickness in AlN films compared to as-deposited films. The oxide thickness is similar on both films with the surface oxidation in as-deposited films increasing slightly more than cycled films at 950°C and 1000°C.

Sputtered films annealed in an ambient environment at high temperatures experience a drastic reduction in film quality which can be determined by the refractive index of the film. AlN exhibiting a refractive index below 1.9 is considered amorphous, whereas polycrystalline AlN has a refractive index from 1.9 to 2.1 and near crystalline is above 2.1. The ellipsometer was used to measure the difference of the refractive index of cycled AlN after annealing. As-deposited films were also measured for comparison and the results are in Figure 4. These films are 350-400 nm thick.

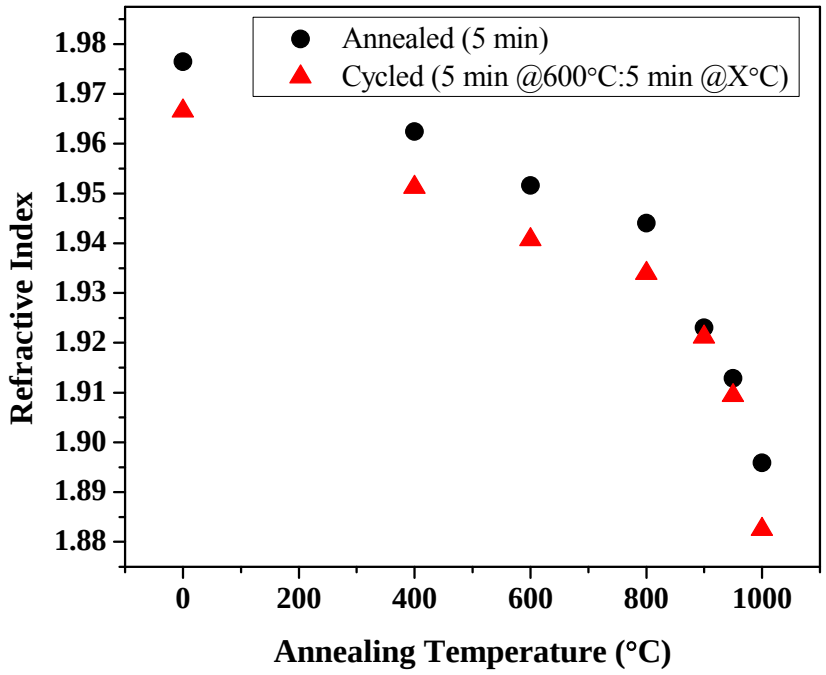

Figure 4 – Refractive index of cycled and as-grown sputtered AlN

The refractive index drastically decreases in both data sets as the film is annealed at higher temperatures indicating that cycling has little effect on the preservation of the quality of the film. In this particular case, the refractive index is actually lower in the cycled film than the as-deposited film after annealing at 1000°C. The results in Figures 3

and 4 illustrate that thermal cycling of sputtered AlN films does not adequately protect them from oxidation in an ambient environment.

Silicon nitride (Si_3N_4) capping was also investigated as a method for protecting AlN films at high temperatures. An Oxford Plasmalab 80Plus plasma enhanced chemical vapor deposition (PECVD) system was used for Si_3N_4 deposition. EDAX was used to measure the atomic % of oxygen in the films after high temperature annealing. Capped films and cycled films were compared against as-deposited films to determine which protection method was more efficient. The results in Figure 5 indicate that capping AlN with Si_3N_4 provides the most protection in an ambient high temperature environment.

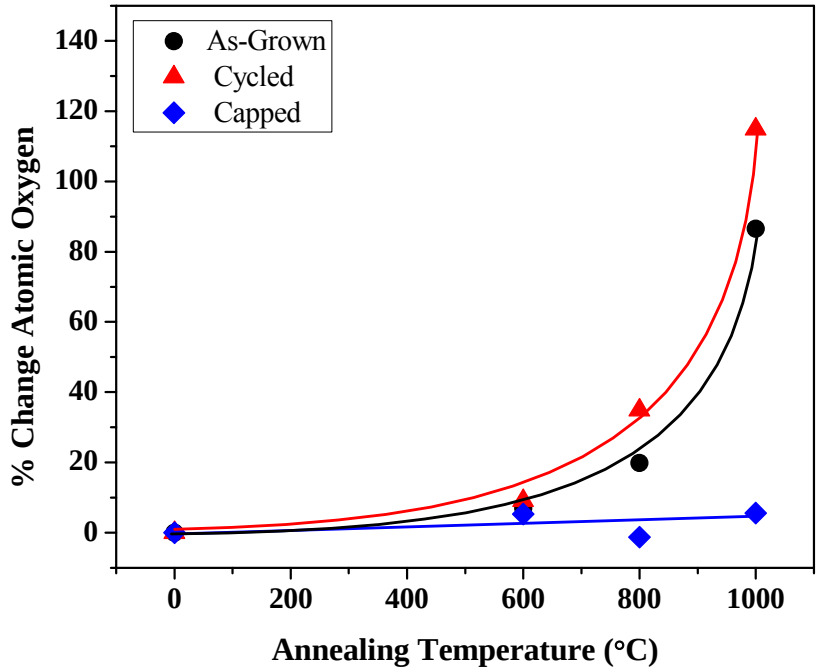

Figure 5 – Comparison of protective methods for AlN

Prior to piezoelectric measurements, MOVPE-grown AlN films were capped with Si_3N_4 and annealed in the RTA for 5 minutes at 1000°C. Pt contacts were deposited post-anneal using a standard photolithography process and Al was deposited on the back of the Si as the bottom electrode. The d_{33} of the uncapped MOVPE-grown films was measured previously using the LDV and the results are in Table 2. This experiment utilizes AlN pieces from the same MOVPE growth to ensure the accuracy of the measurements. The results presented in Figure 6 illustrate the effect of high temperature annealing on the piezoelectric response of AlN films with and without a Si_3N_4 capping layer.

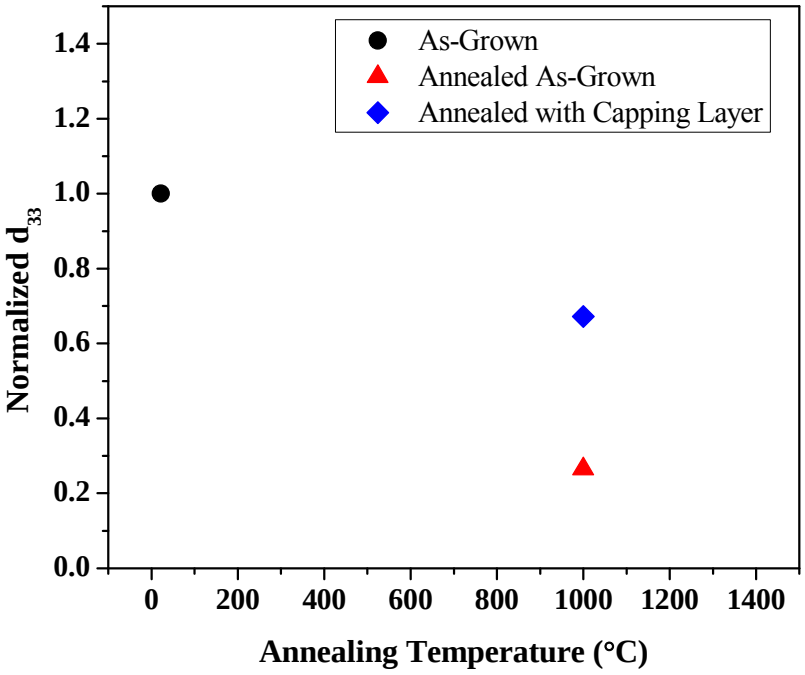

Figure 6 – Annealing effects on capped and uncapped AlN

The data in Figure 6 is presented as the normalized d_{33} to accentuate the drastic reduction in the piezoelectric response of the film as a result of annealing at 1000°C. The d_{33} of the capped film was over 3 times larger than the uncapped annealed film proving that

while there was still a reduction in the piezoelectric response, Si_3N_4 protected the film during high temperature exposure in an ambient environment.

2.4) In-Situ Annealing Study

A high temperature furnace was designed and built that is capable of measuring the d_{33} of sputtered and MOVPE-grown AlN films while annealing the films in a high temperature environment. A basic diagram is provided in Figure 7. The furnace consists of a stainless steel chamber with a 1 inch diameter Al_2O_3 button heater that is rated up to 1200°C and connected to a dc power supply. The sample inside the furnace is electrically probed from an electrical feed-through on the side of the chamber and a gas feed-through allows for the flow of various gasses during high temperature testing. The gas flow rate can be increased up to 20 scfh (approximately 9500 sccm). The top of the furnace has a 1 inch thick 1 inch diameter sapphire view port located directly above the button heater. The temperature is recorded accurately to one tenth of a degree Celsius from a thermocouple which is placed directly against the button heater and connected inside the chamber with another feed-through. The LDV was mounted over the top of the furnace so that the laser travels through the window and onto the sample which is on top of the heater. During room temperature measurements, the AlN sample is 2 cm from the microscope but in this set up the distance is 15 cm, outside the working distance of the microscope. A biconvex 5X magnification lens was mounted between the microscope and the sapphire window on the furnace to increase the working distance of the microscope.

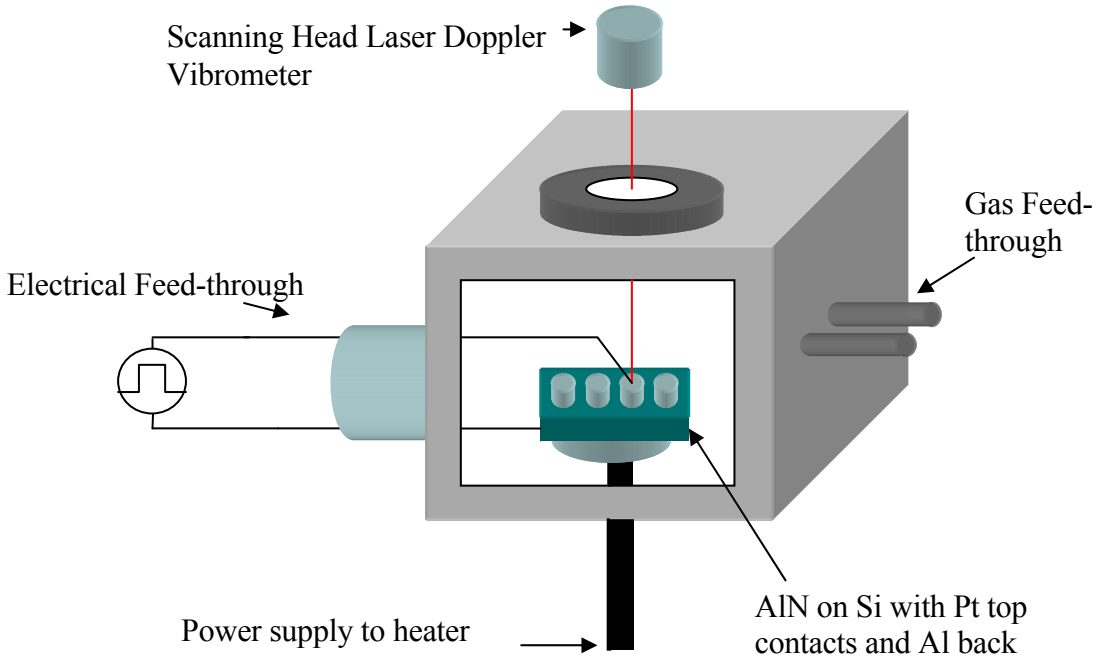

Figure 7 – Diagram of high temperature test chamber

Prior to high temperature testing, sputtered AlN samples were annealed in the RTA in a N_2 environment at 600°C for 1 hour. Annealing the samples prior to in-situ tests assures that no annealing effects of the crystal will be encountered during testing. This preparation is done in a N_2 environment so the films will not oxidize causing a lower d_{33} at the beginning of the measurements. MOVPE-grown films are grown at a much higher temperature than the in-situ testing temperature can reach, so the pre-test annealing preparation is unnecessary for these films.

The largest platinum contacts available to probe on the AlN surface are 400 μm in radius so they cannot be probed directly from the electrical feed-through inside the furnace. A bondpad was designed and fabricated so that probing the contacts is an easier task.

Large Pt contacts (1 cm x 1 cm squares) were deposited onto an insulating Si/SiO_2 wafer using a standard photolithography technique with a thin layer of titanium (~40 nm) used as an adhesion layer. The backside of the AlN test sample was bonded to a large Pt contact (2 cm x 2 cm) on the bondpad using a high temperature silver paste. Then the paste was cured at room temperature for 2 hours followed by a 2 hour 90°C curing bake to ensure maximum adhesion and thermal and electrical conductivity. Gold wire-bonding was used to probe the 400 μm Pt contacts on the test sample from the Ti/Pt contact on the bondpad using a ball-wedge technique. By probing the contacts on the bondpad from the electrical feed-through, the AC signal is relayed to the top and backside of the sample for actuation. A basic diagram of the bondpad is illustrated in Figure 8.

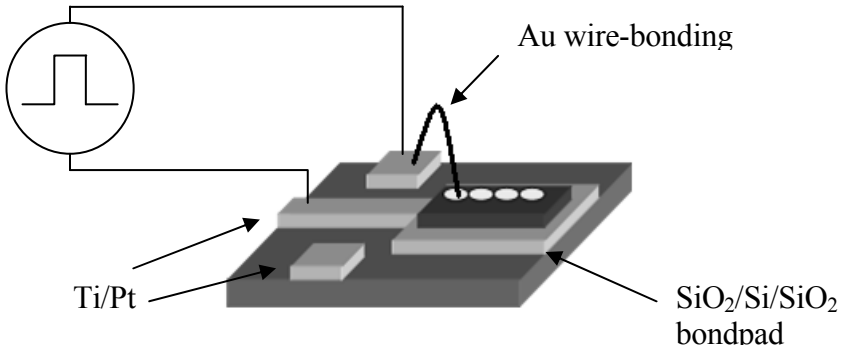

Figure 8 – Bondpad diagram

The furnace is heated by increasing the power to the button heater from the DC power supply. During testing, the temperature of the furnace was increased at a rate of 10°C/minute while N_2 gas was flowing through the chamber at a rate of 2 scfh (approximately 950 sccm). The temperature of the button heater was held to within ±5°C of the target temperature while d_{33} measurements were taken. A 3.5 KHz AC signal was

supplied to the electrical feed-through at varying peak-peak voltages up to 20 V while the picometer level displacement was measured by the LDV. The d_{33} of sputtered and MOVPE-grown films were measured at temperatures up to 300°C. The results of these measurements are summarized in Figure 9.

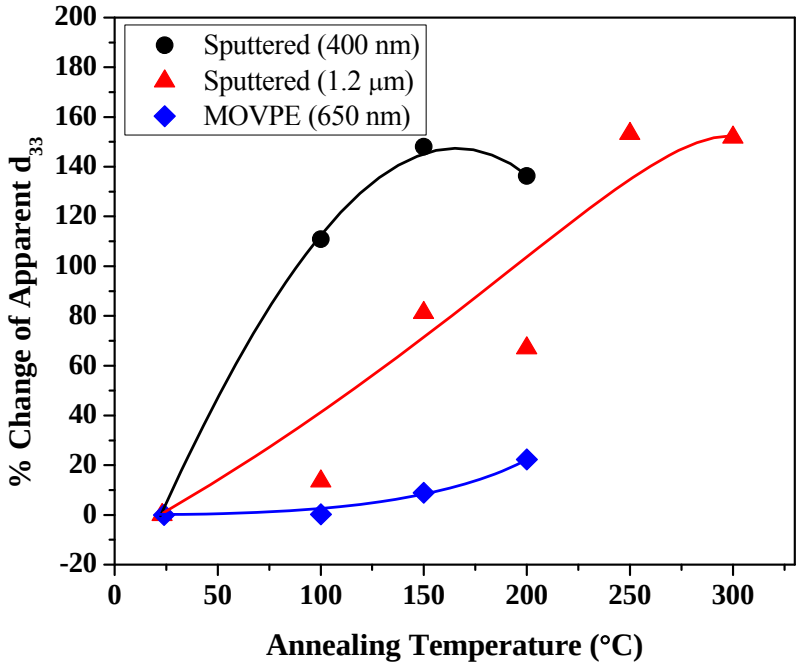

Figure 9 – In-situ piezoelectric response of AlN films

2.5) Discussion

AlN is a robust material with a Curie temperature well above 1000°C but if the film is annealed in a harsh environment, oxidation reduces the piezoelectric response. This work has shown that AlN films oxidize drastically when annealed in an ambient

environment causing a large reduction in the d_{33} of the material. Oxidation and degradation of AlN is caused by a reaction between aluminum and oxygen. This behavior depends on the microstructure of the film. Films exhibiting a columnar microstructure are more optically dense and less susceptible to oxidation than films with a granular microstructure. The oxidation trends in Figures 1 and 2 shows that oxidation of sputtered films increases more at higher temperatures than MOVPE-grown AlN which is consistent with literature [34].

If the films are protected from oxidation, the d_{33} of the material may be preserved up to 1000°C. Methods used in this study to protect the films from oxidation while retaining the original piezoelectric response were cycling and Si_3N_4 capping. Cycled films were annealed up to 600°C then cooled prior to annealing again at temperatures as high as 1000°C. Ellipsometry measurements show that surface oxidation was only slightly reduced compared to films simply annealed at 1000°C and the refractive index was not preserved. EDAX results verified that Si_3N_4 capping is a more effective method of protecting AlN films from harsh environments. Unprotected annealed films and cycled films both exhibited an increase in the percentage of oxygen in the film at high temperatures while the oxygen content in capped films remained constant. The piezoelectric response of an MOVPE-grown AlN film was measured and compared against the d_{33} measured in a capped film and an uncapped film exposed to 1000°C in an ambient environment. The d_{33} of the uncapped annealed film was drastically reduced while the capped film retained 66% of the original d_{33} of the as-grown unannealed film. The reduction of d_{33} in the capped annealed film could be attributed to the quality of the PECVD-deposited Si_3N_4. The

capping layer was deposited at 300°C and was not heat treated after deposition so the Si_3N_4 layer was not very dense thus more susceptible to decomposition at 1000°C. Si_3N_4 is a rigid non-piezoelectric ceramic so the drop in electric field over the capping layer or the rigidity of the layer could also be factors in the reduction of piezoelectric response from the capped annealed AlN films.

A high temperature test chamber was designed and built and in-situ piezoelectric measurements of sputtered and MOVPE-grown AlN films were taken at temperatures up to 300°C. It is evident that there is an increase in the measured d_{33} as the annealing temperature increased. The piezoelectric response in the sputtered films nearly doubled while the response in the MOVPE-grown film gradually increased. AlN is a pyroelectric material with a calculated pyroelectric coefficient between 6 – 8 $\mu C/(m^2K)$ [35]. However, this effect can be disregarded because the induced charge as a result of pyroelectricity is produced as a function of change in temperature with time ($\delta T/ \delta t$) and the measurements in this experiment were taken at a constant temperature [36]. Any fluctuation of temperature during these measurements was minimal (± 1 - 5°C) which would result in a negligible induced charge that contributes mV to the AC signal used to actuate the sample (~125 mV in a 500 nm film during a 5°C change in temperature).

The increase in the measured d_{33} could be caused by the difference in thermal expansion coefficients between AlN and Si. At 100°C, the thermal expansion coefficients of Si and a-plane AlN are roughly 3.57×10^{-6}/°C and 4.15×10^{-6}/°C, respectively [37]. At high temperatures, the AlN film expands more than the Si substrate, decreasing the lattice

mismatch allowing the AlN layer to behave more like an unclamped film. However, a more detailed study of clamped and unclamped AlN films, including in-situ measurements of the d_{33}, will need to be conducted to verify these trends.

At temperatures higher than 200°C, the thin sputtered AlN films become conductive and when the temperature is decreased to room temperature, these previously insulating films still conduct. This was not seen in films that had been annealed in the RTA prior to d_{33} measurements. During ex-situ testing, AlN films were annealed at 1000°C prior to measurements and AlN films used for in-situ tests were pre-annealed at 600°C. None of these films were conductive when room temperature measurements were taken leading to the conclusion that the application of an electric field across the sample at high temperatures causes dielectric breakdown. Thicker sputtered films (~1200 nm) did not break down until 300°C. The apparent relationship between the thickness of the film and the temperature at which the film becomes conductive also indicates dielectric breakdown. Figure 9 only shows d_{33} data from the MOVPE-grown AlN (~600 nm) film up to 300°C because the laser from the LDV continuously lost intensity as the films were actuated at high temperature. This could be a result of bending in the films due to thermal expansion causing the laser to reflect in an arbitrary direction. Although the laser signal was lost, the MOVPE-grown films were actuated while annealed at temperatures higher than 300°C to test the dielectric limits of the film. The film broke down at 400°C leading to the conclusion that a film with a poor crystalline quality may be more susceptible to dielectric breakdown at high temperatures.

CHAPTER 3: ALN ETCH CHARACTERISTICS

3.1) Motivation

Most MEMS devices are comprised of 3D structures requiring patterning by etching. Controlled wet and dry etching for patterning device structures is an important requirement for application of AlN and related materials. Etch rate, selectivity, and isotropy are important factors in considering different etching techniques. Wet etching generally is more selective while dry etching is more anisotropic producing nearly vertical sidewalls without undercutting the masking material. The etch rate of a material depends on many factors related to the parameters used in the wet or dry etching technique and may depend on the quality of the material. Wet and dry etching of AlN is explored in this chapter for the purpose of fabricating 3D MEMS actuators which are discussed later in this work.

3.2) Wet Etching Background

Wet etching of AlN in acidic and basic solutions has been studied in depth. A variety of solutions, such as hot HF/H_2O [38-40], HF/HNO_3 [41], or NaOH [42], can be used to etch sputtered amorphous AlN. Mileham *et al* noticed during photolithographic processing that the developer solution they were using (AZ400K) produced substantial

etching in their polycrystalline AlN films as well [43]. The active ingredient in the developer solution is potassium hydroxide (KOH) which is perfectly selective for AlN over both GaN and Al_2O_3. This group measured the time dependence of the etch depth of the AlN films and determined that there is a linear dependence concluding that the etch rate is dependent on the etchant concentration which is characteristic of a rate-controlled etch. Heating up the solution increased the isotropic etch rates causing significant undercutting of the masking material.

Polarity is another factor in AlN that affects etching rates in KOH solutions. Schowalter *et al* observed that the Al-face is chemically more stable than the N-face in KOH solutions [44] which has also been observed in GaN. Zhuang *et al* noticed a similar trend as Mileham *et al* while measuring the time dependence of the etch rate of KOH solutions at room temperature. The rate decreased over time, but Zhuang *et al* suspected that the decrease in etch rate was due to the depletion of the easiest etched crystal planes and not a result of etchant depletion at the sample surface [45]. It was concluded that the etch rate decreased with time as the crystal planes exhibiting Al-polarity were exposed to the etchant.

While a variety of wet etch solutions have been employed for amorphous and polycrystalline AlN (the most selective and controllable being KOH), none to date have been proven for etching single-crystal AlN. Wet chemical etching with a KOH-based solution is strongly dependent on the crystal quality – defect density, grain size, and polarity – of AlN [46]. Experiments by Cimalla *et al* have shown that high quality MBE-

AlN deposited on sapphire cannot be etched at room temperature. A very slow lateral etch is detected indicating pronounced defect-related etching along threading dislocations. The same group reports that sputtered AlN on Si exhibited a fast etch rate while metalorganic chemical vapor deposited (MOCVD) AlN on Si and on Al_2O_3 exhibited slower etch rates [47].

3.3) Dry Etching Background

Wet etching of AlN using KOH-based solutions has the advantage of controllable, selective and isotropic etching of polycrystalline films. Higher-quality films, however, exhibit a much lower etch rate and only etch among thread defects and grain boundaries with little detectable vertical etching. In the case of AlN, wet etching may not be sufficient depending on the crystal quality of the material. Dry etching is anisotropic and optimal for structures with small feature sizes.

Various plasma etch techniques such as reactive ion etching (RIE), electron cyclotron resonance (ECR), inductively coupled plasma (ICP), and reactive ion beam etching (RIBE) have been used to etch III-nitrides. In an ECR system plasmas are formed at low pressures with low plasma potentials and ion energies. The samples are not exposed to intense discharge like in an RIE system so there is not as much damage to the film. Alternatively, ICP systems form a high density plasma by applying rf-power to an inductive coil encircling a dielectric vessel. The coil produces an electric field inducing a

strong magnetic field in the vertical plane trapping electrons in the center of the chamber producing a high density plasma. At pressures lower than 20 mTorr the plasma diffuses from the center of the chamber to the substrate at low ion energy producing minimal damage and high etch rates. ECR and ICP etch systems produce the highest etch rates and smoothest morphologies in group-III nitrides. The high plasma density systems improve the bond-breaking efficiency and enhance sputter desorption of etch products from the surface of the material. While the etch characteristics are similar, ICP systems are more widely used than ECR because ICP systems are easier to scale-up than ECR sources and are more economical [50].

Reactive ion etching (RIE) using an inductively coupled plasma (ICP) is a versatile form of dry etching in which the conditions may be optimized to produce an anisotropic etch profile and minimize surface roughness. An etching gas should be chosen that reacts with the material that is to be removed. Choosing the right gas mixture is important because the reaction products should be volatile. Etch rates are often limited by the group-III halogen etch product, therefore high volatility etch products such as chlorine-, iodine-, and bromine-based solutions are preferred to etch Al-containing materials as compared to fluorine-based solutions [48].

While dry etching group-III nitride materials in a chlorine-based gas mixture, the excited material interacts with exposed regions of the material while the ions in the plasma physically bombard the sample and remove etched material. The vertical etch rate depends on both the chemical and physical etch but the etch rate is not the sum of the two quantities.

Ions bombarding the surface of the material often remove reaction products from the surface of the sample, allowing fresh reactants to reach the surface, increasing the etch rate. Also, excited species striking the material may weaken bonds within the lattice allowing the chemical removal to proceed more easily. This is important because AlN has a large bond energy of 11.52 eV/atom [49]. Choosing the proper reactant gases, ICP coil power, RIE power, and plasma pressure controls the etch rate, selectivity, and rms roughness of the etched film.

Shul *et al* studied the etch rates and selectivity of group-III nitrides using an ICP-generated BCl_3/Cl_2 plasma. The effects of gas chemistry, ICP coil power, rf-bias, and pressure on the etch rate of group-III nitrides were investigated. The plasma conditions in their experiment were 2 mTorr pressure, 32 sccm Cl_2, 8 sccm BCl_3, 5 sccm Ar, and 500 W ICP coil power. They found that AlN etch rates increased with increasing Cl_2 concentration in the plasma up to 40% Cl_2 then remained relatively constant. The slower etch rate in comparison to GaN was be attributed to the strong bond density in AlN (11.52 eV/atom) compared to GaN (7.72 eV/atom). Adjusting the cathode rf-power was used as a method of changing the chemical-to-physical component of the etch mechanism by varying the energy of the ions which bombard the substrate. The etch rate of AlN increased with increasing rf-power which was attributed to more efficient bond-breaking and sputter desorption of the etch products caused by the more physical etch mechanism. The ICP power was also be changed to adjust the chemical-to-physical component of the etch mechanism. Increasing the ICP power creates a purely chemical etch reducing the energy of the ions used in the physical etch mechanism [49].

3.4) Wet Chemical Etching

MOCVD-AlN was grown on GaN on a sapphire substrate because the small lattice mismatch is necessary to grow highly crystalline material. Actuation of the piezoelectric film requires the electric field to be isolated over the AlN material. Because the underlying substrate (Al_2O_3) is a thick insulator, the film cannot be actuated conventionally by sputtering a metal contact on the backside of the sample. Therefore, the AlN film must be masked and etched down to the GaN layer which can be doped with Si during growth to create a conductive layer.

Buffered oxide etch (BOE) is a hydrofluoric acid (HF)-based solution that is sometimes used to etch polycrystalline or amorphous AlN. HF reacts with oxides so defects in an amorphous crystal structure allowing the sample to oxidize at room temperature make the material easily etched with BOE. The crystalline AlN film was masked with a hardened layer of photoresist and dipped in BOE for 25 minutes. The height of the photoresist mask was measured prior to etching with a stylus profilometer then measured again after the sample was dipped in the BOE solution. The measurement showed no change in the height of the photoresist mask indicating the film had not been etched.

A KOH-based solution was used in the next attempt to etch the crystalline AlN film grown on GaN. The same type of photoresist mask was used to protect the areas of the

AlN film that were not meant to be etched. The KOH-based solution had a KOH concentration of 11% by weight and was heated to 80°C prior to etching. After 25 minutes in the KOH-based solution, the photoresist was removed using a photoresist stripper, and the height of the etched wells was measured with the stylus profilometer. The photoresist pattern was evident on the surface of the film, indicating some lateral etching of AlN, however no vertical etching was detected.

3.5) Etch Characterization of Sputtered AlN

The uniform crystallinity of the MOCVD-AlN film grown on GaN made the film nearly impossible to etch using conventional wet etching methods. Dry etching methods using Cl_2-based inductively coupled plasma (ICP) would be needed to etch the high quality material. A Trion Mini-Lock Phantom III Series ICP-RIE system was used for this study. The samples were mounted using carbon tape onto a 3-inch Si wafer which was clamped to the cathode and cooled with He gas. The test samples used for this etch characterization were masked using carbon paint which is etch-resistant in the Cl_2/BCl_3 gas mixture and soluble in acetone. After the carbon paint was removed, the etch rates were calculated using an alpha-step stylus profilometer. The samples were etched for 3 minutes each and the depth measurements were taken at a minimum of 3 positions.

A thorough study was conducted to determine how the etching parameters of the ICP system affected the etch rate of AlN. High quality sputtered films and MOVPE-grown

films were of particular interest for this study. The high quality sputtered AlN films were etched using different RIE powers to observe the effect on the sidewall profile. A scanning electron microscope (SEM) was used to produce the pictures of the sidewall profile shown in Figure 10. Prior to etching, the film was masked with Ni in a striped pattern using a standard photolithography technique. The samples shown in Figures 10a, 10b, and 10c were etched using RIE powers of 100 W, 150 W, and 200 W respectively in a BCl_3/Cl_2 gas chemistry. The plasma parameters were 400 W ICP power, 20 mTorr pressure, 15 sccm BCl_3, and 15 sccm Cl_2.

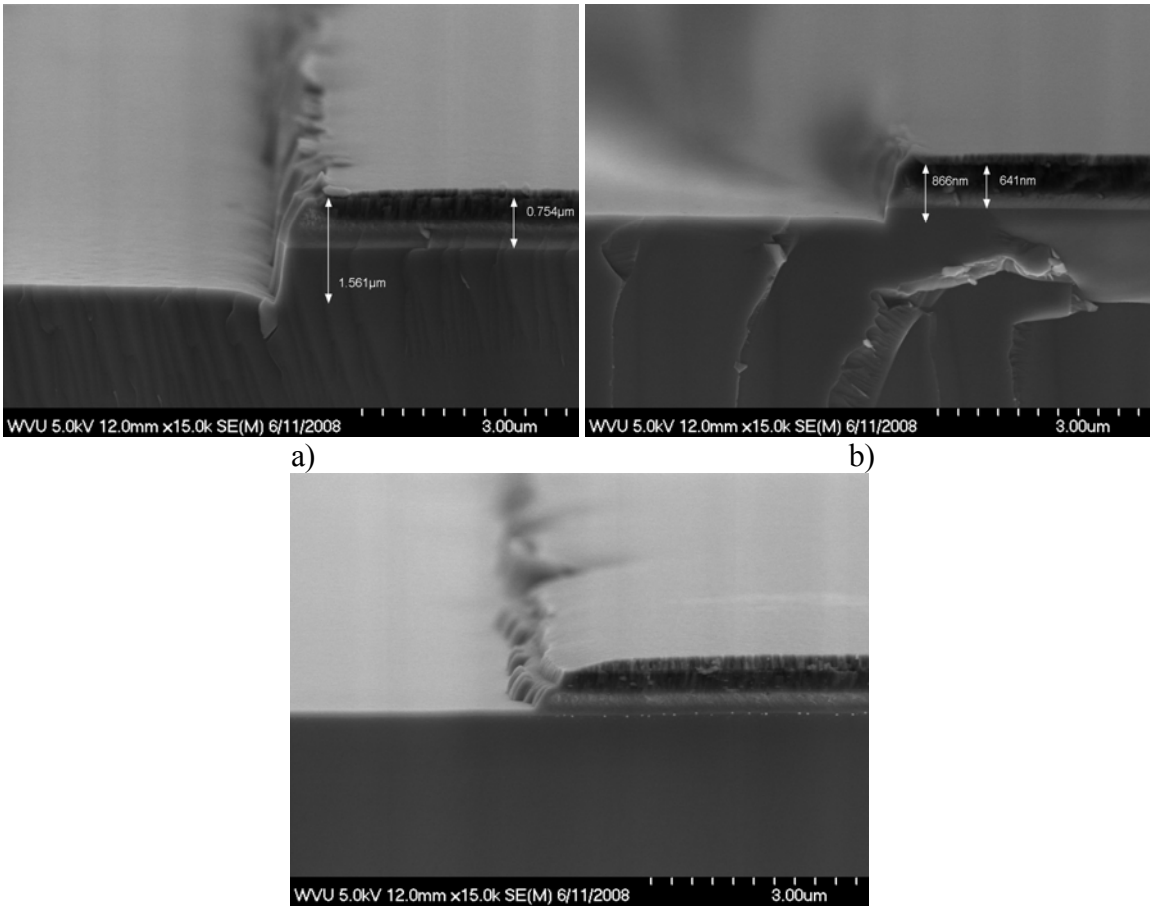

a) b)

c)

Figure 10 – Sidewall profile of AlN etched at different RIE powers

The images in Figure 10 indicate nearly vertical sidewalls can be achieved while etching at RIE powers of 100 W and 150 W. Etching with 200 W resulted in rough sidewalls possibly due to the increase of the physical etch mechanism at high RIE powers. The features that are sought for this application are rather large (hundreds of microns) so the difference in sidewall profile between 100 W and 150 W is negligible for this study.

AlN was deposited onto a Pt electrode using a high power density sputtering technique. The reasons for this setup will be made clear in subsequent chapters. A thorough study of the relationship between the etch rate of AlN and the etching parameters was carried out to further understand the nature of this material. Figures 11 and 12 illustrate the effects of the RIE and ICP power on the etch rate of AlN, respectively. By adjusting the RIE and ICP powers, the chemical-to-physical component of the etch mechanism can be changed. Increasing the RIE power while leaving all other parameters constant increases the physical etch component. The etch rate of the AlN sample increased with increasing RIE power up to 100 W due to more efficient bond breaking and sputter desorption of etch products at higher ion energies. Above 100 W the physical component dominated the etch mechanism and the etch rate began to decrease as a result of sputter desorption of particles that have not had a chance to react with the surface of the sample. For the measurements taken in Figure 11, the rest of the plasma conditions were 400 W ICP power, 20 mTorr pressure, 15 sccm BCl_3, and 15 sccm Cl_2.

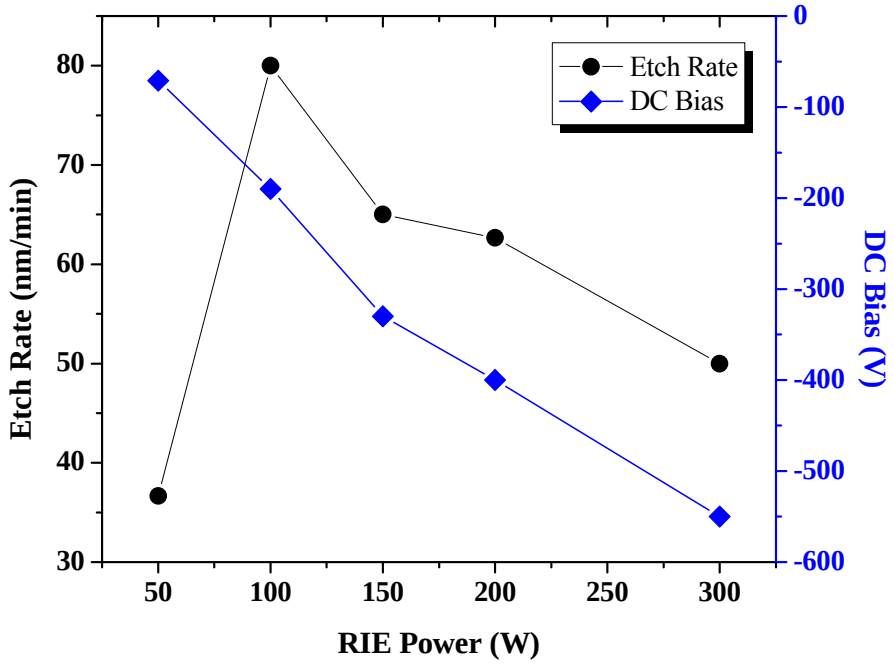

Figure 11 – Etch rate of sputtered AlN as a function of RIE power

The ICP power effects the chemical component of the etch mechanism by changing the plasma density. As a function of increasing plasma density, etch rates typically increase due to higher concentration of reactive neutrals and higher ion flux which increases the bond breaking efficiency of AlN [51]. At 0 ICP power (not shown), the etch rates were negligible. As the ICP power increased from 0 W, the etch rate increased up to 400 W, then decreased up to 900 W ICP power. The observed decrease at higher source power can be attributed to saturation of reactive neutrals at the sample surface or sputter desorption of Cl_2 prior to its reaction with the surface of the AlN film. At 900 W, the etch rate was actually negative, indicating that the chemical reactions were taking place faster than the physical ion bombardment was sputtering the etch products away. The plasma

conditions used while varying the ICP power in Figure 12 were 100 W RIE power, 20 mTorr pressure, 15 sccm BCl_3, and 15 sccm Cl_2.

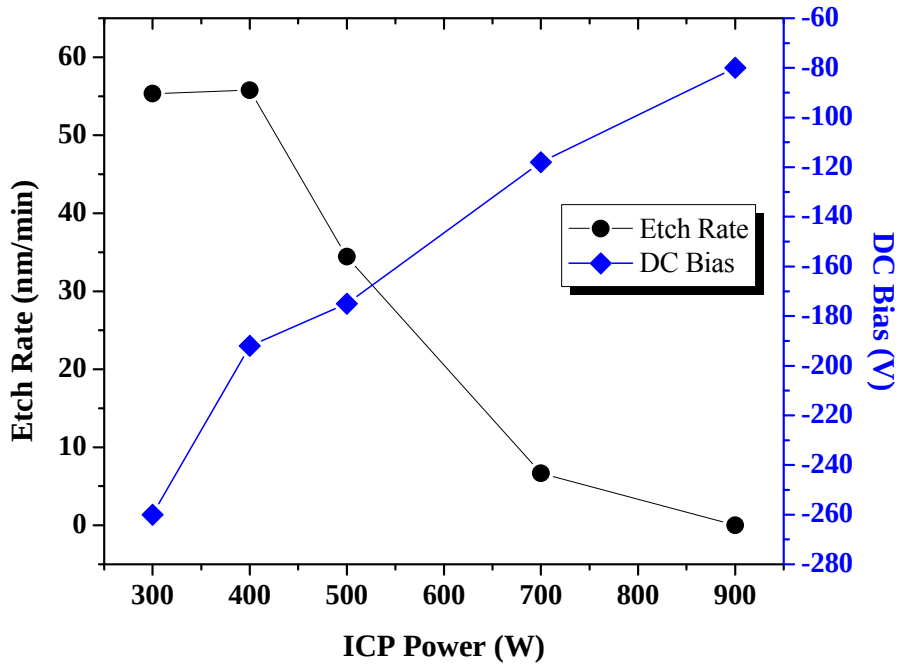

Figure 12 – Etch rate of sputtered AlN as a function of ICP power

Another way to adjust the physical-to-chemical component of the etch mechanism is to change the concentration of the reactive component in the gas mixture. Figure 13 illustrates the effect of Cl_2 concentration in the gas chemistry on the etch rate of AlN. As the Cl_2 concentration was increased, the etch rate increased due to higher concentrations of reactive Cl atoms. Some studies have shown a decrease in the etch rate of AlN with a gas composition of 100% Cl_2 due to less efficient sputter desorption of etch products away from the surface of the material [49-52]. However, it is clear from Figure 13 that the chemical component is a dominant factor in this experiment. It is important to note that the presence of heavier BCl_3 molecules is often used to improve the surface roughness of

etched AlN films so using a pure Cl_2 gas mixture will not result in optimal film properties [52].

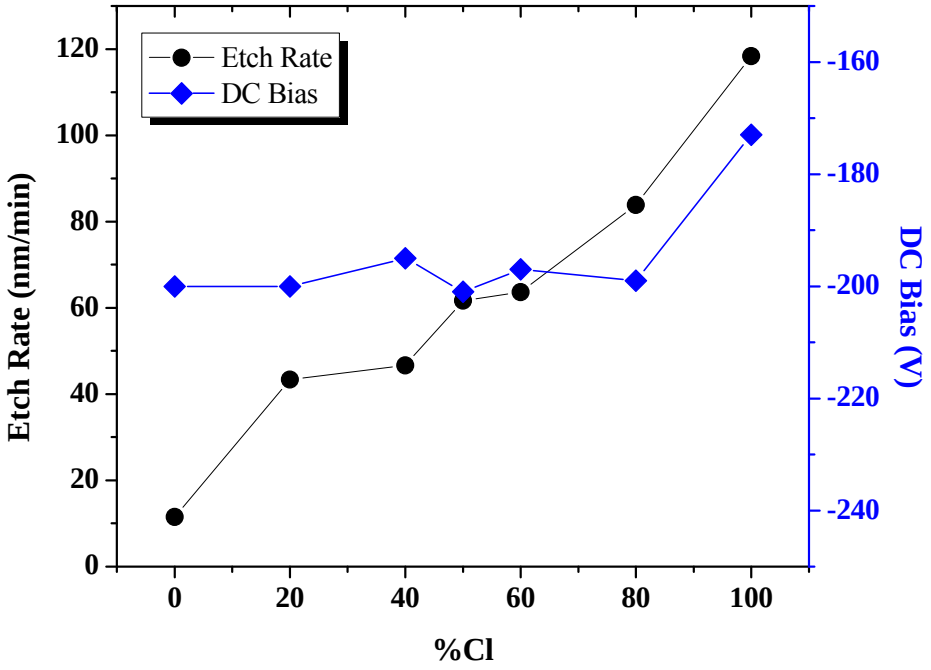

Figure 13 – Etch rate of sputtered AlN as a function of $\%Cl_2$

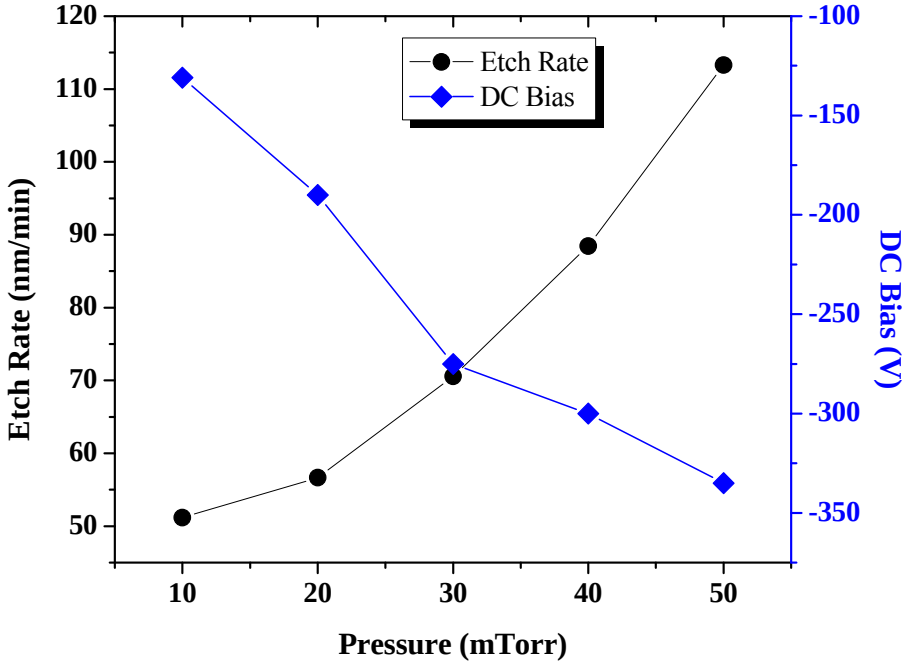

Figure 14 – Etch rate of sputtered AlN as a function of pressure

Most reported studies on the etch characteristics of III-nitrides vary the chamber pressure at values less than 10 mTorr, however the limit of this TRION ICP system is 10 mTorr so for the purposes of this study, the pressure was varied from 10 mTorr to 50 mTorr. The etch rate increased as the pressure increased which contradicts the data reported in literature when extrapolated to 50 mTorr [49-51]. Plasma conditions change dramatically as a function of pressure, in particular the mean free path decreases and the ion flux increases as the pressure is increased. Literature reports that low pressures aid the directionality of the ion flux yielding excellent anisotropy and etch rates of AlN [52]. It is possible, however, that the high etch rate observed at higher pressures in this experiment result from an increased ion flux. The increased concentration of reactive molecules in the high density plasma may result in faster etch rates at higher pressures.

The etch rate of AlN films increased with increasing dc-bias which corresponds closely to ion energy. Ion energies influence the physical component of the etch mechanism by improving the bond breaking efficiency and sputter desorption of reactive materials. For the ICP system used in these experiments, the dc-bias is dependent on the plasma conditions and cannot be set manually.

3.6) Etch Characterization of MOVPE-grown AlN

MOVPE-grown AlN on GaN is a crystalline material impervious to wet etching in KOH-based solutions so dry etching in Cl_2-based plasma is necessary. An etch characterization study similar to the study involving sputtered AlN was carried out. Figures 15 and 16 exhibit the effect of RIE and ICP power on the etch rate of AlN, respectively.

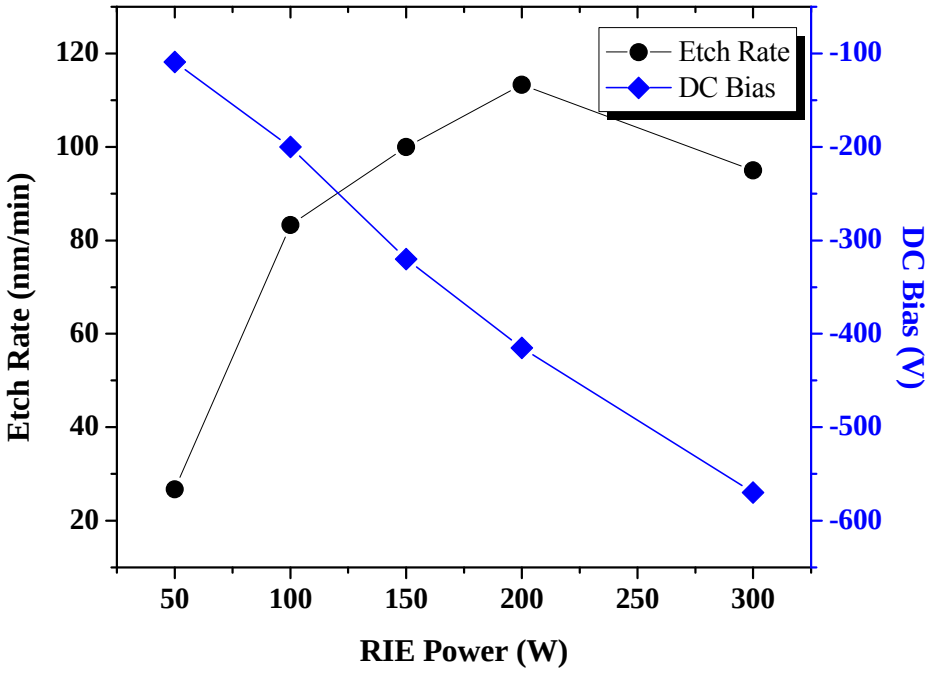

Figure 15 – Etch rate of MOVPE-grown AlN as a function of RIE power

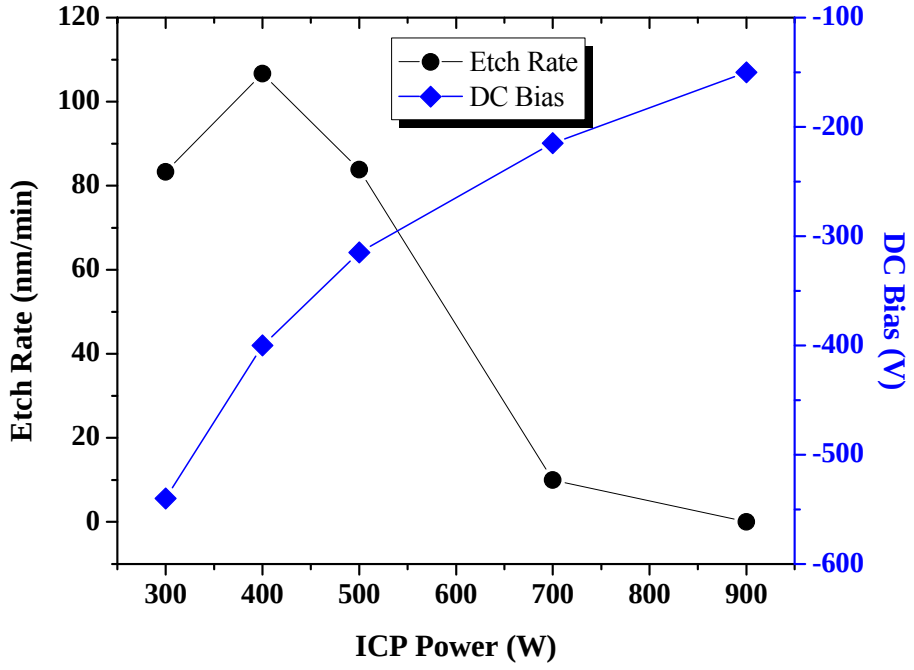

Figure 16 – Etch rate of MOVPE-grown AlN as a function of ICP power

The etch rate increases as a function of RIE power up to 200 W then decreases at 300 W. The maximum etch rate was found in the MOVPE-AlN at a higher RIE power than the sputtered AlN indicating the higher quality film required a more physical component in the etch mechanism. The decrease in the etch rate at 300 W is a result of the physical bombardment sputtering volatile products away from the surface before they react with the AlN. For the remainder of the etch characterization study of MOVPE-grown films, the RIE power was set to 200 W with the other plasma parameters set to 20 mTorr pressure, 400 W ICP power, 15 sccm BCl_3, and 15 sccm Cl_2. The etch rate in Figure 16 increased as the ICP power increased up to 400 W before gradually decreasing, exhibiting the same trend as the sputtered AlN film. Above 400 W, the saturation of reactive neutrals on the surface of the material slows the etch rate.

Figure 17 illustrates the change in etch rate as a function of % Cl_2 in the BCl_3/Cl_2 gas mixture. As in the previous study, the etch rate increases as the Cl_2 concentration in the gas chemistry increases up to 100%. The change is not as dramatic in this study and the difference in the etch rate between 50% Cl_2 and 100% Cl_2 is small. The etch rate levels off at high Cl_2 concentrations due to the saturation of reactants on the surface of the material.

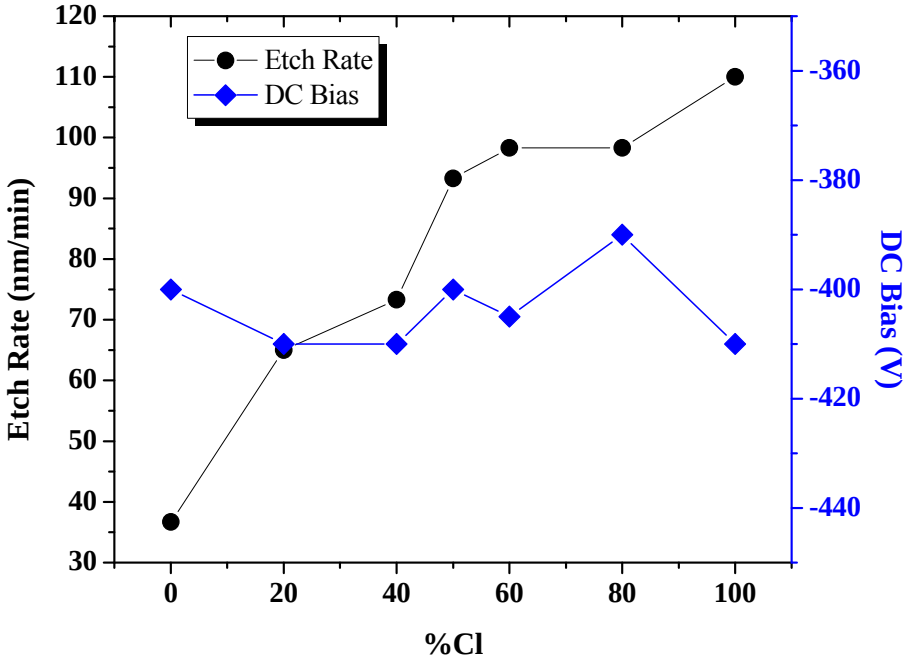

Figure 17 – Etch rate of MOVPE-grown AlN as a function of $\%Cl_2$

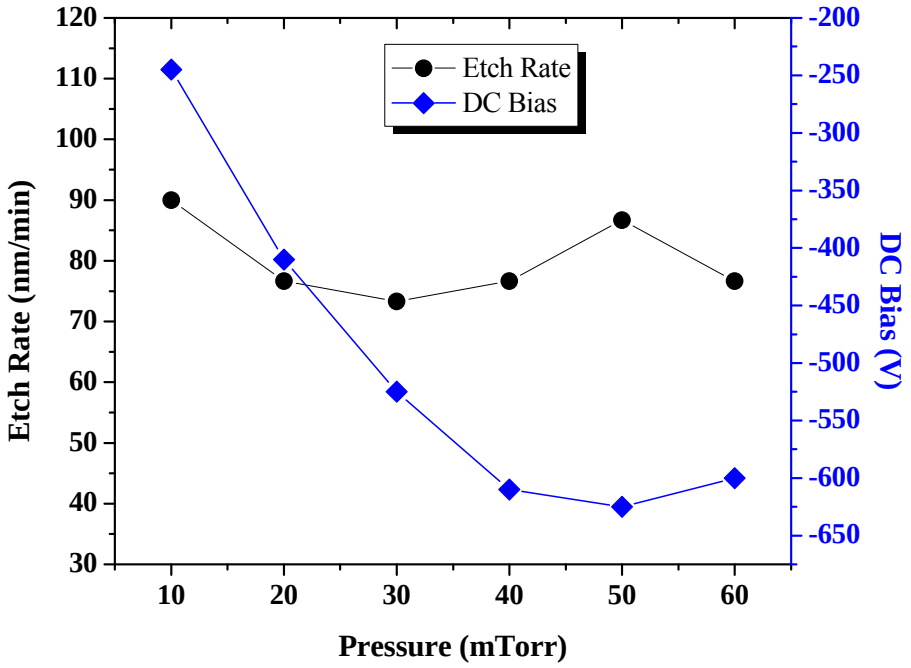

Figure 18 – Etch rate of MOVPE-grown AlN on GaN as a function of pressure

There is some fluctuation in the etch rate at different chamber pressures. The high etch rate at low chamber pressures is consistent with what is reported in literature. Increasing the pressure increases the Cl ion and neutral molecules present in the chamber so the chemical etching mechanism is increased. However, it is reported that the positive ion flux is reduced at higher chamber pressures reducing the etch rate [52]. The crystalline nature of the MOCVD-AlN grown on GaN requires a more physical etching mechanism as shown in Figure 15. At higher chamber pressures the physical bombardment may be reduced due to the reduction in mean free path and increase in volatile surface reactants that may not be sputtered away fast enough.

3.7) Discussion

Wet chemical etching is a great technique for isotropic and selective etching however it is not the best method for etching high quality AlN. The etch rate of AlN in a KOH-based solution strongly depends on the crystal quality of the material. Amorphous AlN is etched must faster than MOVPE-AlN on Si, while crystalline AlN cannot be etched in KOH at all.

ICP high density plasma etching systems produce high etch rates with minimal damage to the sample surface. Etch characterization of sputtered AlN and MOVPE-AlN grown on GaN were carried out to determine how the plasma parameters affect the etch rate of AlN. Adjusting the RIE power, ICP coil power, and gas chemistry, the chemical-to-

physical component of the etch mechanism can be changed changed. The high quality MOVPE-AlN grown on GaN required a more physical etching mechanism than sputtered AlN, however the etch rate also increased with increasing Cl_2 concentration in the gas mixture indicating that the etch rate is dependent on the chemical component as well. A delicate balance between the plasma parameters must be sought to produce optimal features on the etched material. With plasma conditions of 100 W RIE power, 400 W ICP power, 20 mTorr pressure, 15 sccm BCl_3, and 15 sccm Cl_2, the etch rate of sputtered and MOVPE-grown AlN was ~80 and ~66 nm/min, respectively.

CHAPTER 4: ALN MESA STRUCTURES

4.1) Motivation

Aluminum nitride (AlN) films have been explored for piezoelectric and high temperature microelectromechanical systems (MEMS) applications but few device geometries have been explored in depth. One of the main advantages of using AlN as an active material is its ability to retain piezoelectric properties at high temperatures. Typically, a metal layer covering the entire AlN film is used as a top electrode in d_{33} measurements [32]. In this chapter, the effect of different contact metals and contact geometries on the measured piezoelectric response of the film is studied and the fabrication techniques used to make these structures are described. The piezoelectric response of the 3D structures is then compared to the response of an AlN film deposited directly onto a platinum electrode.

4.2) Development of Sputtered AlN Mesas

AlN mesa structures are fabricated to isolate the d_{33} piezoelectric coefficient by reducing the effect of non-normal electric field lines on the piezoelectric response of the film. Figure 19a illustrates the emergence of non-normal field lines in AlN thin films when a voltage is applied to the top and bottom electrodes. Figure 19b shows how the AlN mesa

structure reduces the non-normal field lines reducing the contribution of the lateral displacement in the film caused by the d_{31} piezoelectric coefficient. This configuration also allows for better confinement of the electric field and therefore more accurate d_{33} measurements.

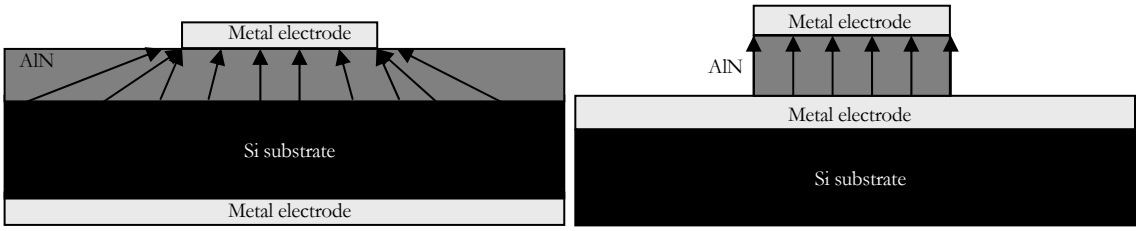

Figure 19 – Diagram of electric field lines in AlN a) films and b) mesas

Two types of sputtered AlN films were investigated as discussed below; low power density sputtered and high power density sputtered. DC reactive sputtering was used to deposit polycrystalline AlN using an Al target with an Ar/N flow of 3/27 sccm in a CVC 610 dc magnetron sputtering station. The quality of the material can be changed by adjusting the power density and chamber pressure during the sputter deposition. Low power density depositions produce AlN films with a refractive index of ~1.9 which indicates nearly amorphous crystal quality.

AlN mesas sputtered with low power density were fabricated using a bottom up approach. The heat from the sputter deposition is relatively low at low power densities so a photolithography technique can be utilized. A thin layer of metal is sputtered onto a clean Si wafer then a standard negative photolithography process is performed to create a photoresist mask with openings down to the metal layer. AlN is deposited with an 8" Al

target at 500 W under a pressure of 30 mTorr then a metal layer is deposited on top. After a standard liftoff technique, what remains are AlN mesa structures with metal contacts on top with a thin metal layer underneath.

The bottom-up fabrication approach cannot be used to make mesa structures from higher quality AlN (refractive index ~2.0-2.05). The higher sputtering power density generates too much heat causing the photoresist mask to burn so a top-down approach to the mesa fabrication had to be implemented. A thin metal is first sputtered onto a Si wafer followed by a highly c-axis oriented AlN film sputtered with the parameters outlined in Table 3.

Table 3 – Sputtering conditions for amorphous and polycrystalline AlN

Parameters	Amorphous AlN	Polycrystalline AlN
Al Target (%)	99.999	99.999
Target Size	8” diameter	2” diameter
DC Power (W)	500	200
Substrate Temperature	Room Temperature	Room Temperature
Sputtering Pressure (mTorr)	30	45
Sputtering time (minutes)	50	50
N_2 concentration (%)	99.999	99.999
Ar/N_2	3/27	3/27

The same negative photolithography technique is used to create a photoresist mask with openings down to the AlN layer then metal is deposited. After liftoff, what remains are metal contacts on an AlN film on top of a metal layer. After mask realignment, a positive photolithography technique is used to create a reversal of the photoresist mask used to deposit metal contacts, so there is a thick layer (~5 μm) of AZ 4400 photoresist covering the metal contacts on the AlN film and the rest of the film is exposed. Finally, a dry etch of AlN is performed using an Inductively Coupled Plasma (ICP) system with Cl_2/BCl_3 gas chemistry using the conditions outlined in Table 4. The exposed AlN film is etched down to the bottom metal layer and an Asher process using an O_2/CF_4 chemistry is used to rid the sample of the photoresist mask.

Table 4 – Plasma conditions used to etch AlN

Plasma Conditions	AlN Etch	Asher
RIE Power (W)	100	25
ICP Power (W)	400	500
Gas Mixture	BCl_3/Cl_2	O_2/CF_4
Gas Flow	15/15 sccm	45/5 sccm
Pressure	20 mTorr	100 mTorr

4.3) Piezoelectric Characterization of Sputtered Mesa Structures

Combinations of Pt and Al were used as the top and bottom electrodes and the apparent effect of contact material on the piezoelectric response was investigated. The top

electrode refers to the metal deposited on top of the AlN mesa and the bottom electrode refers to the contact metal deposited underneath the AlN mesa. In Figures 20 and 21, "Pt/Al" refers to a Pt top and Al bottom contact combination and so on. An MSV-100 Polytec scanning head laser Doppler vibrometer (LDV) was used to measure the picometer displacement of the AlN mesas while applying an AC signal at a frequency of 3.5 kHz. The results of the sputtered low quality AlN mesas and higher quality AlN mesas can be seen in Figures 20 and 21, respectively.

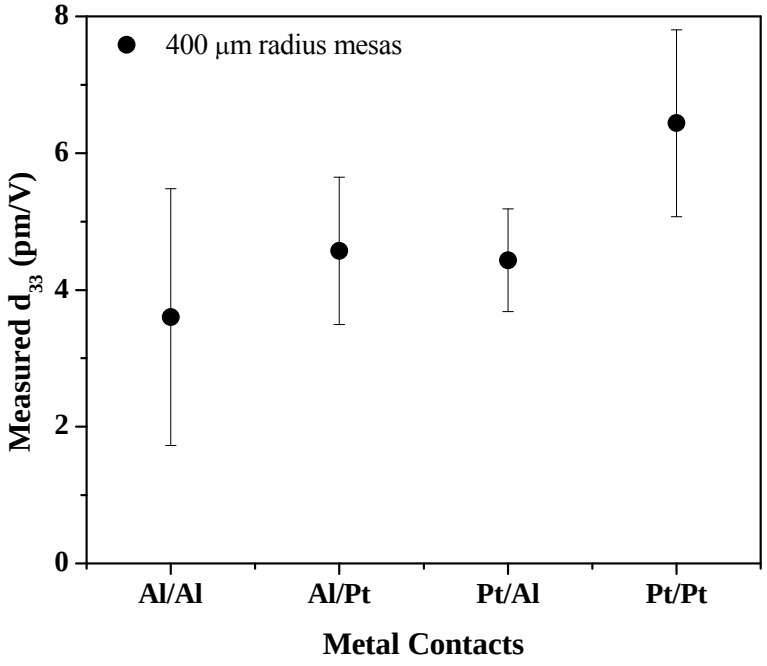

Figure 20 – Bottom-up fabricated amorphous AlN mesas

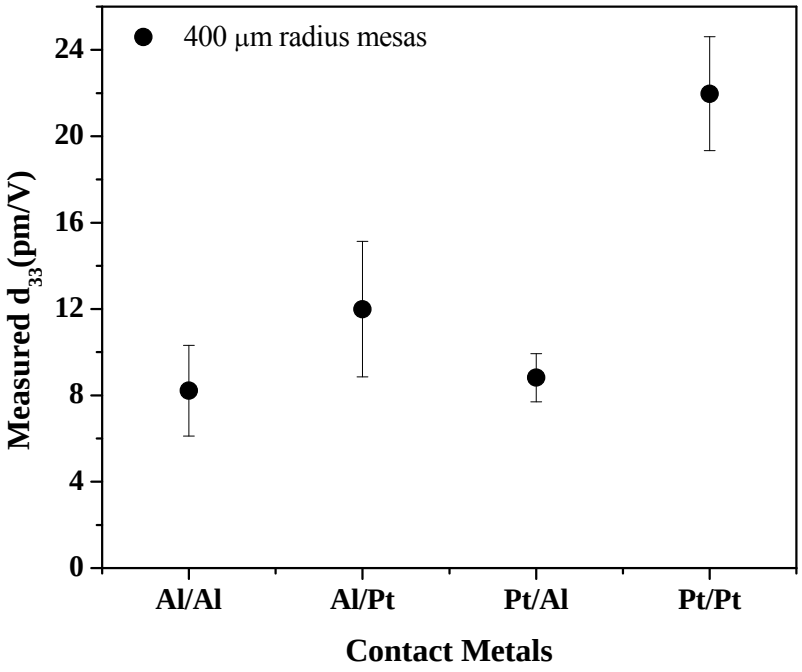

Figure 21 – Top-down fabricated polycrystalline AlN mesas

The measured piezoelectric response of the mesa structures fabricated using both techniques shows a similar trend with Pt/Pt contact combination exhibiting the highest measured d_{33} value on average. The results displayed in Figures 20 and 21 were all taken from 400 μm radius mesas. Measurements were taken to determine whether mesa size has a relationship with the piezoelectric response and Figure 22 plots responses of different metal contacts and different mesa sizes to show that the measured piezoelectric response of the AlN mesas is dependent on both contact material and 3D geometry.

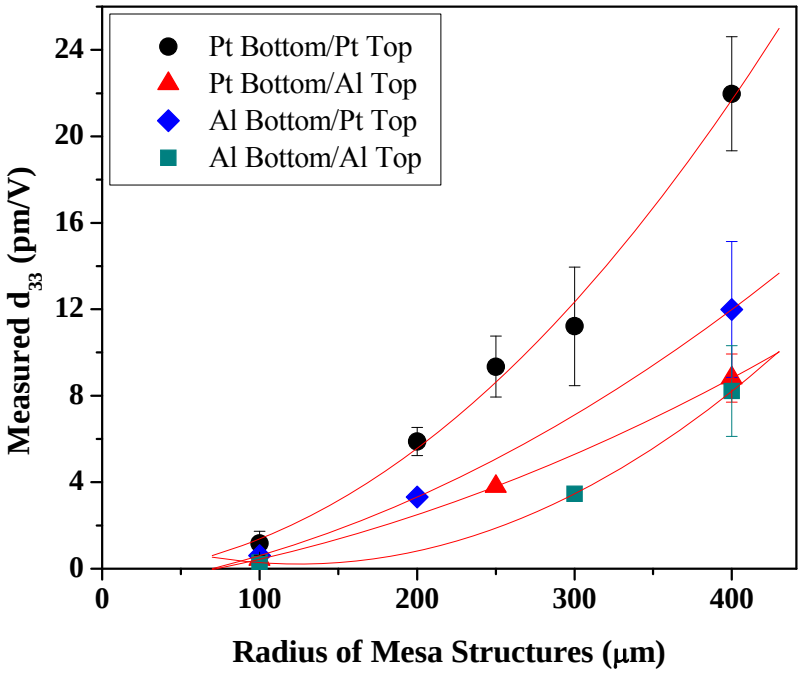

Figure 22 – Piezoelectric response of different-sized mesa structures

The piezoelectric response of the mesas increases with increasing radius and the response from mesas with different metal contacts exhibits the same results seen in Figures 20 and 21. The Pt/AlN/Pt combination displayed the largest response (as large as 22 pm/V) and the Al/AlN/Al configuration displayed the smallest. As the mesa size increases, the response of the mesas increases at a nearly parabolic rate indicating a strong dependence on the surface area of the structure. The Pt/AlN/Pt contact configuration on the high quality sputtered AlN mesas are the focus of the rest of this study.

Measurements were taken at different positions on mesas with different radii to determine if the piezoelectric response is uniform across an entire structure (Figure 23). The measurements were taken along the diameter of the mesa and the first and last

measurement for each mesa was taken at a position off the side of the mesa on the substrate material to show that the response of the mesa structure is significant enough to cause vibrations elsewhere in the sample. The 400 μm radius mesa exhibits a larger piezoelectric response in the center and a smaller response at the edge. The smaller response at the edge of the mesa structures may be due to oxidation of the exposed vertical AlN sidewall. The asher process which etches the photoresist mask is an oxygen-based plasma which may oxidize the exposed AlN. The piezoelectric response at the center of the mesa is more pronounced in larger structures because the edge effects are local to the outside of the mesa allowing the center of the mesa to move more freely. In smaller mesa structures, the edge effects are more dominant which restricts the movement of the center of the structures.

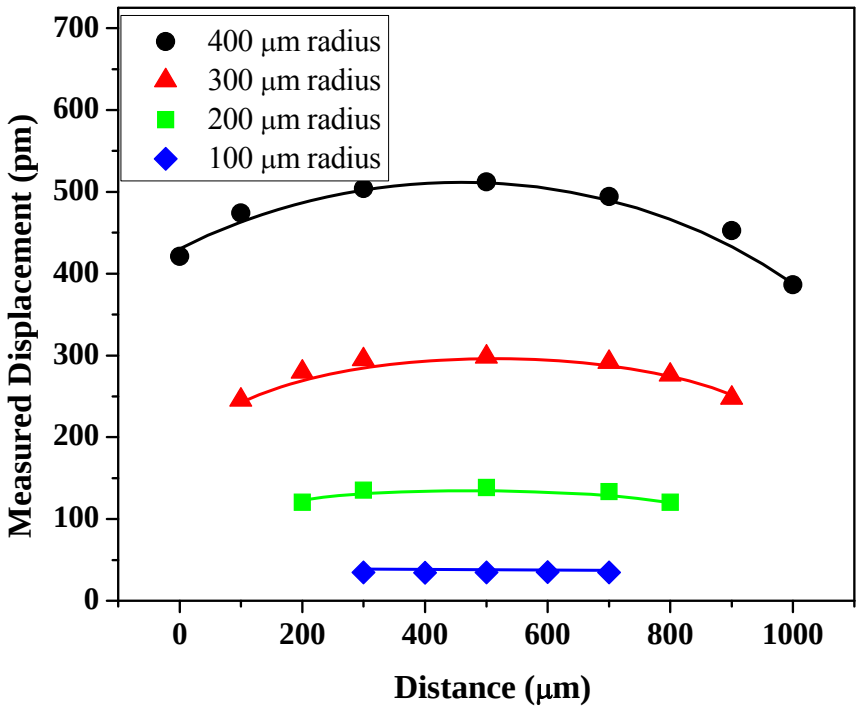

Figure 23 – Piezoelectric response along the diameter of mesa structures

To ensure the large measured displacement in the AlN mesas is not an artifact of resonance, the frequency response of mesas of different sizes and with different contact metals was measured. Figure 24 displays the frequency response of mesas with different radius.

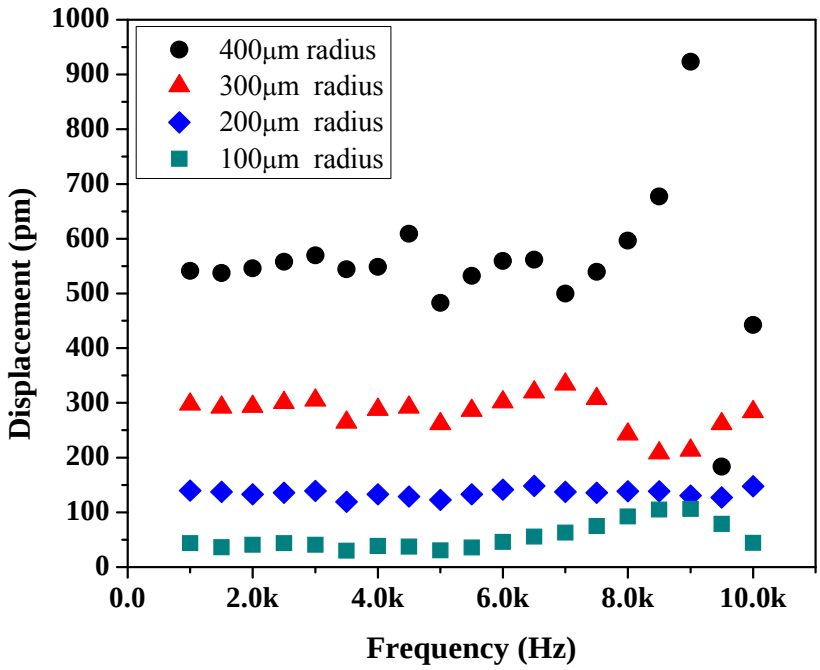

Figure 24 – Frequency response of different-sized mesas

The results of the frequency response in Figure 24 show that actuation at low frequencies has little effect on the response of the mesas. Above 7 kHz, frequency has more of an impact on the displacement of the mesas. The frequency response of mesa structures with different metal contacts is displayed in Figure 25. The results are similar to those in Figure 24 where the observed piezoelectric displacement is relatively consistent at lower frequency values then varies above 8 kHz. The piezoelectric dependence on contact

material is also observed in this study. The frequency dependence (Figures 24 and 25) shows that there is no resonance at the probing frequency (3.5 kHz).

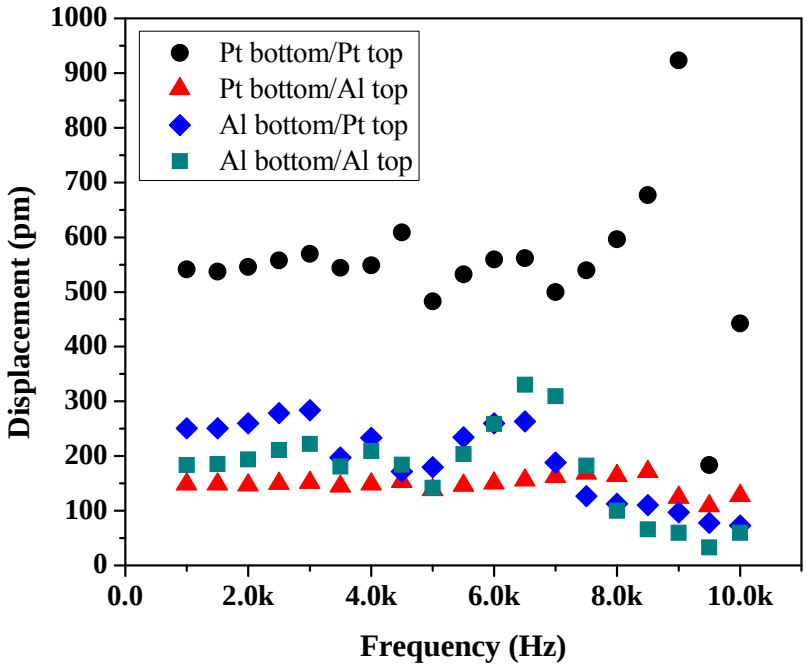

Figure 25 – Frequency response of mesas with different contact metals

The MSV-100 Polytec (LDV) is capable of scanning over a large area and mapping the piezoelectric response at different points in a user-defined scan area. These measurements show how AlN responds at different points on different sized mesas. Figures 26a, 26b, 26c, and 26d show the LDV surface mapping results of 400 µm, 300 µm, 200 µm, and 100 µm radius contacts, respectively.

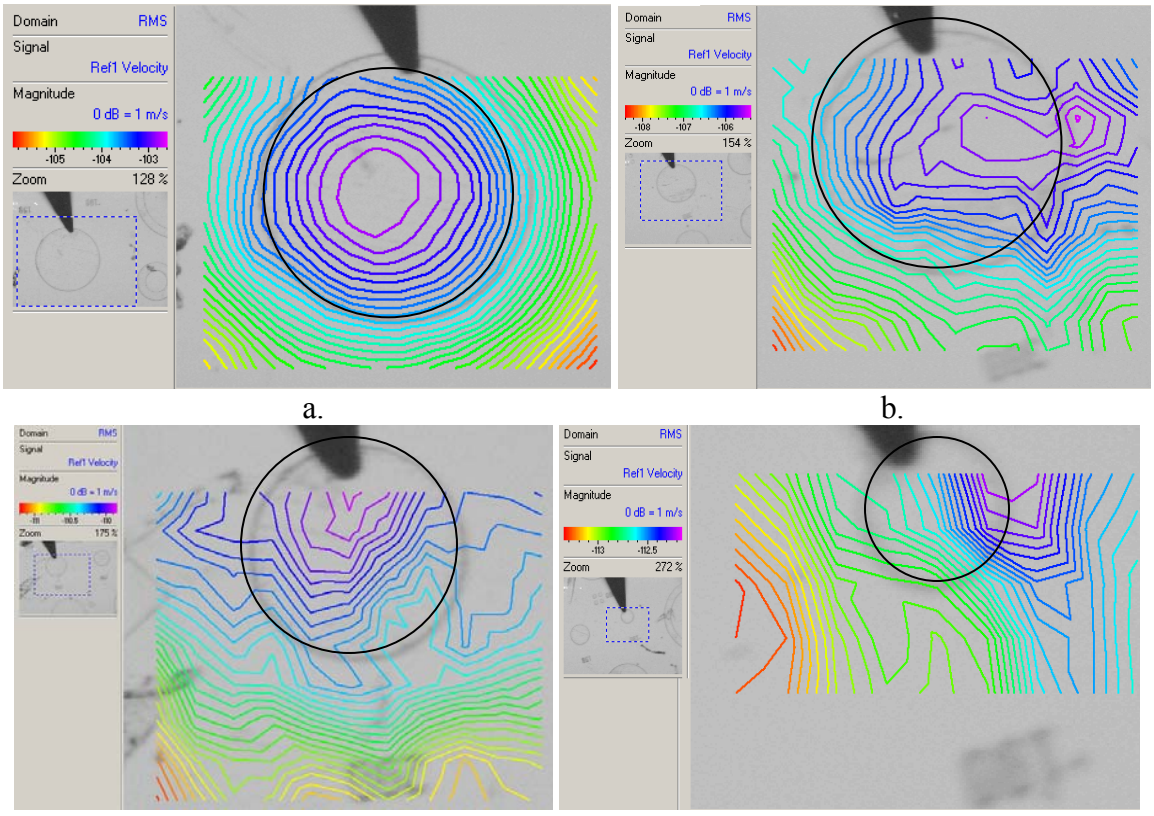

Figure 26 – Distribution of piezoelectric response in mesas

The surface scans in Figure 26 display the dB magnitude of the velocity of the AlN mesas over a designated area. The 400 μm radius mesas exhibit the highest response in the center with a gradual decrease in response extending out to the area of the sample where no AlN is present. The mesas in Figure 26 are outlined with a darkened circle. The smaller sized mesas exhibit a different trend, where the highest response is not in the center of the mesa and the isolines are not evenly distributed. This result is not intrinsically understood and is still under investigation.

4.4) MOVPE-grown AlN Mesas

MOVPE-grown AlN was used in the study of mesa structures because of the high crystalline quality of the material and controllable growth conditions. AlN grown on GaN is of particularly high crystalline quality due to the small lattice mismatch between AlN and GaN. Reflection high energy electron diffraction (RHEED) was used to show the crystallographic properties of the sample surface. Figure 27 shows the diffraction pattern of the MOVPE-grown AlN film. The dots indicate a highly crystalline material because of the uniform constructive and destructive interference of the reflected electron beam. If the film was of poor crystal quality, rings would be present in the diffraction pattern.

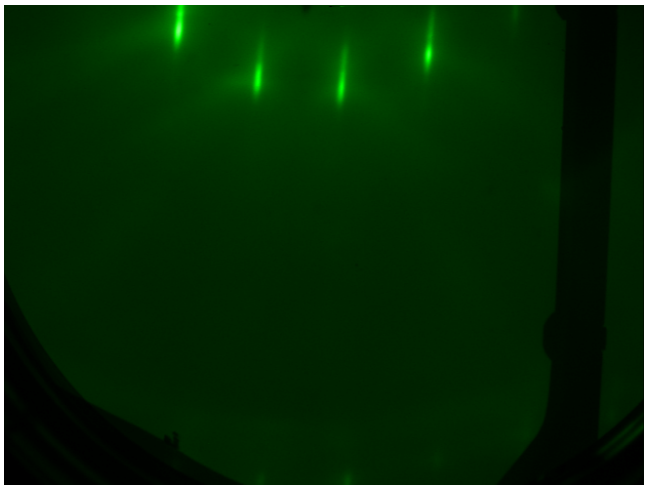

Figure 27 – RHEED results of MOVPE-AlN grown on GaN

The GaN layer was heavily doped with Si to provide a conductive layer under the AlN to act as the bottom electrode when mesa structures are fabricated. Doping the GaN layer causes strain in the crystal structure which leads to cracking. Since the AlN is highly crystalline and the lattice mismatch is small, cracking in the GaN causes cracking in the

AlN film as well. The scanning electron microscope (SEM) picture in Figure 28 shows cracking in the GaN, AlN and even the Pt contact on top of the etched AlN mesa structure.

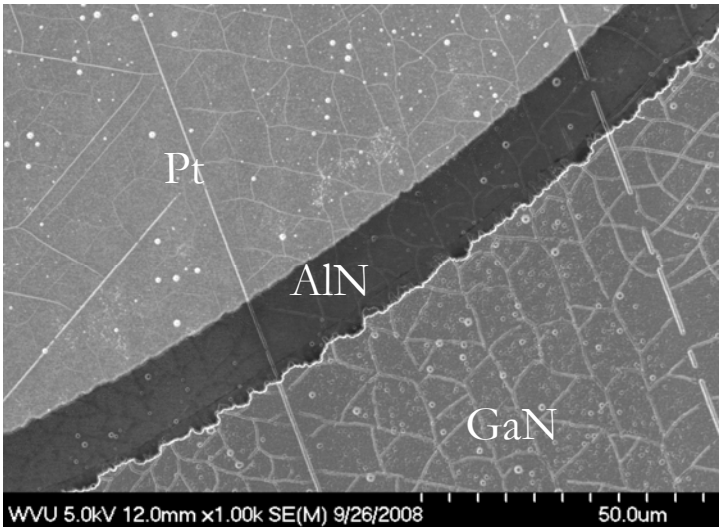

Figure 28 – Bird's-eye view of a cracked mesa structure

Fabrication of mesa structures using MOVPE-grown AlN was similar to the top down fabrication method employed for higher quality sputtered films. Metal contacts were deposited on the AlN film using a standard negative photolithography process. Then, using a positive photolithography process, the contacts were masked with AZ 4400 photoresist to protect the metal during etching. The film was etched in the ICP system using the same conditions described in Table 4. An Asher process removed the AZ 4400 photoresist mask after etching. A platinum contact pad was deposited onto a portion of the film that had been etched down to the conductive Si-doped GaN layer. Platinum and aluminum were used as metal contacts on top of the mesa structures and Ti/Al was deposited on GaN because it creates an ohmic contact with the GaN layer.

LDV measurements of the first set of mesas fabricated from the MOVPE-grown AlN on Si-doped GaN were unsuccessful because the mesa structures were conducting. The cracks in the AlN layer allowed for the deposited metal contacts to fill the cracks causing the films to conduct when the AC signal was sent to the top metal contact and GaN. To solve this problem, a new set of mesas was fabricated using SiO_2 as a buffer layer between the top metal contact and the cracked AlN. A thin layer of PECVD-deposited SiO_2 was put over the cracked AlN film prior to the metal contact deposition. After photolithography, the metal contacts were sputtered on the SiO_2 layer and the sample was placed in hydrofluoric (HF) acid to etch away the SiO_2 that was not covered by metal. After mask realignment, the AZ 4400 photoresist was used as a mask as described earlier in this chapter and etching proceeded using the same technique.

The SiO_2 buffer layer prevented some of the mesas structures from conducting when the AC signal was applied. There was still conduction in some of the mesa structures possibly due to the thickness of the SiO_2 layer (~50 nm) or the low quality of the buffer layer resulting from the PECVD deposition. The SiO_2 layer was deposited at a low temperature (100°C) to reduce the possibility of oxygen diffusion into the AlN and GaN layers of the mesas. Preliminary results obtained from LDV can be seen in Table 5.

Table 5 – Piezoelectric response of MOVPE-grown AlN mesas

Topside Metal Contact	d_{33} (pm/V)	Error (pm/V)
Al	5.456	1.421
Pt	5.508	2.593

4.5) Films vs. Mesa Structures

The large error bars displayed in the previous section gave reason to believe that the observed piezoelectric response of the AlN mesas may vary across a particular sample due to differences in film thickness and/or crystal quality. The contact mask used during photolithography techniques throughout the experiments up to this point has same-sized circular contacts spaced far apart making it difficult to map the d_{33} across the entire film. The mask also produced merely 8-10 measurable same-size contacts on a 1 cm x 1 cm sample, not nearly enough to make accurate conclusions about the average piezoelectric coefficient (d_{33}) and observed trends over an entire sample. A new contact mask was designed for mapping the piezoelectric response across a film using many same-size contacts. The experiment conducted in this section utilized the capabilities made available by the new mask design to map the d_{33} across an entire sample. The design of this new mask is described in detail in Appendix A.

The goal of the following experiment was to measure the piezoelectric response of an AlN film then to etch the film and measure the piezoelectric response of the mesa structures. By measuring the apparent d_{33} the film then mesas over the exact same area of AlN, the residual effects of the AlN film (non-normal electric field lines and lateral d_{31} contribution) on the piezoelectric response will be known. Using the new contact mask allows for a higher number of contacts to measure which should decrease the overall error in measurements and produce a more accurate average d_{33} value.

Typically, measuring the d_{33} of an AlN film requires the bottom electrode to be deposited on the backside of a doped Si wafer. For this experiment, however, the end result is AlN mesas on a Pt electrode, so AlN film deposition must be on a layer of Pt. This Pt layer will be probed as the backside contact for measuring both the film and mesa structures. High quality AlN was sputtered using a 2" Al target using the high power density technique described in Table 3. During AlN film deposition, an area of the deposited Pt layer was masked to ensure that there was an opening to the backside of the film. Then a standard negative photolithography technique was used and circular Pt contacts were deposited on the surface of the AlN film. A diagram of the top and side view of the AlN film prepared for LDV measurements is shown in Figure 29.

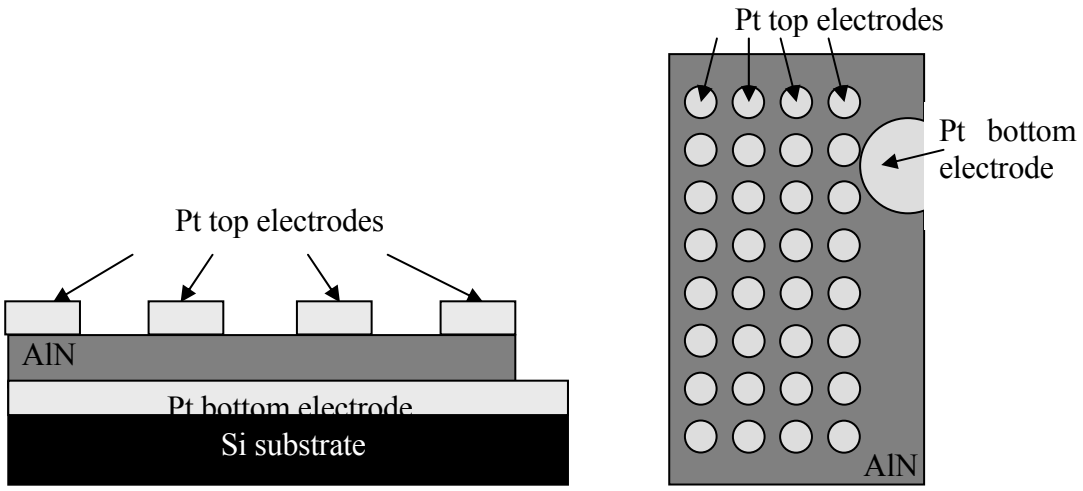

Figure 29 – Side and top view of AlN film

The portion of the film that was masked during AlN deposition leaves an opening to probe the entire Pt film beneath the AlN layer. The top electrodes are probed one contact at a time. It was expected that there would be non-normal electric field lines and

contribution from the transverse piezoelectric coefficient (d_{31}) that may reduce the measured piezoelectric response normal to the surface of the film. Etching to form mesa structures should isolate the d_{33} piezoelectric coefficient and normal electric field lines enhancing the piezoelectric response. Piezoelectric characterization was done using the LDV. Each contact was probed with an AC signal propagating at 3.5 kHz at values of 2 V, 4 V, and 6 V peak-to-peak and the 3D map of the results are displayed in figure 30. The gray areas in the 3D map indicate areas on the film that reached dielectric breakdown so no piezoelectric measurements could be taken.

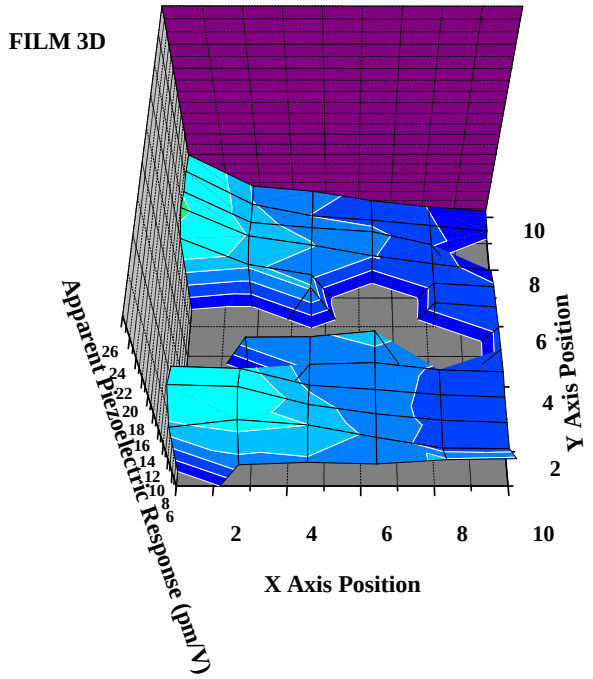

Figure 30 – 3D map of the piezoelectric response of an AlN film on Pt

After measurements were taken on each contact of the AlN film, mesa structures were fabricated using dry etching. A positive photolithography technique was used to

create a mask with AZ4400 photoresist covering each Pt contact on top of the AlN film and the films were etched using the parameters listed in Table 4. Each mesa was probed individually with an AC signal as described previously and the piezoelectric response was measured using the LDV. The 3D surface map of the piezoelectric response of the mesas is exhibited in Figure 31.

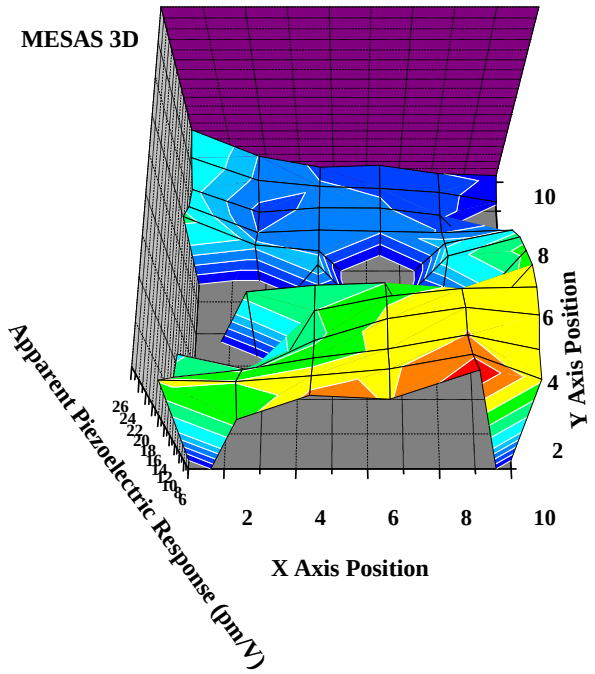

Figure 31 – 3D map of the piezoelectric response of AlN mesas

The piezoelectric response of the mesa structures showed an increase in over 50% of the areas measured prior to mesa fabrication. The highest piezoelectric response exhibited by the mesa structures was over 25 pm/V.

4.6) Discussion

Sputtered AlN mesa structures have been fabricated using a bottom-up and top-down approach with different metals used for top and bottom contacts. The Pt/Pt contact combination exhibits the highest measured piezoelectric response in mesa structures fabricated using both techniques which is consistent with literature [16]. The residual stress in the metallic thin films was not directly measured in this study; however there is reportedly no correlation between the stress caused by the AlN/electrode mismatch (10.9% for Pt) and the measured d_{33} value. Pt exhibits properties of symmetry similar to sapphire providing an optimal nucleation surface for AlN deposition resulting in more crystalline films and a large piezoelectric response [15].

AlN was grown on GaN in an MOVPE system and mesas were fabricated using the top-down fabrication technique. The low piezoelectric response (Table 5) relative to the sputtered mesas could be a result of the SiO_2 buffer layer increasing the rigidity of the film or decreasing the electric field drop over the AlN layer. The cracks in the sample cause a discontinuity across the film and SiO_2 that is deposited in the cracks may be limiting the motion of the AlN film as well.

From the results in Figure 30, it is clear that the piezoelectric response varies across a sputtered AlN sample. This may be due to a variation of thickness or crystal quality across the film. The lighter colors in Figures 30 and 31 indicate a larger piezoelectric

response in that area of the sample. The films were etched to form mesa structures and piezoelectric measurements were taken over the same areas of the AlN sample to compare the response of mesa structures vs. films. The piezoelectric response increased in over 50% of the mesa structures fabricated when compared to measurements of the film. This indicates that the mesa structures are successful in isolating normal electric field lines and the d_{33} piezoelectric coefficient. The reason the piezoelectric response remained the same in some areas of the sample is not yet understood and requires further investigation.

CHAPTER 5: CONCLUSIONS AND FUTURE WORK

High temperature testing was performed on AlN films and the annealing effects on the piezoelectric properties were reported. Films were annealed in a rapid thermal annealing (RTA) system and the oxygen % (atomic) was measured using energy dispersive X-ray analysis (EDAX). EDAX results indicated that sputtered films oxidized faster than MOVPE-grown AlN films due to the difference in crystal quality; however both films oxidized at extremely high temperatures (1000°C). Si_3N_4 was found to protect AlN from oxidation at high temperatures better than thermal cycling. Si_3N_4-capped films annealed at 1000°C preserved 66% of the film's original piezoelectric response. The uncapped annealed films only preserved 25% of the film's original response. A more efficient means of protecting the AlN film while preserving the piezoelectric response must be investigated in the future. Ideally, 100% of the original piezoelectric response would be preserved after annealing.

A high temperature test chamber was built and in-situ high temperature piezoelectric measurements of AlN films were taken. The piezoelectric response of the films increased with increasing temperature likely due to the different thermal expansion coefficients of AlN and Si changing the internal stress of the film. The films exhibited dielectric breakdown after a voltage was applied at high temperatures. Thin sputtered films broke down at 200°C, thick sputtered films at 300°C and the MOVPE-grown AlN film broke down at 400°C. In the future, the effects of substrate material on the increased

response at high temperature should be studied. If AlN films deposited on Pt exhibit a different response than with the Si substrate, it can be concluded that the substrate material and possibly the thermal expansion coefficient has a significant effect on the observed trends. The effects of the measurement technique on the dielectric breakdown should also be investigated. Applying a voltage to the sample at high temperatures causes the film to conduct so there may be an issue with the bondpad design or measurement technique. Some research groups using the indirect piezoelectric measurement technique report the piezoelectric response of AlN up to 300°C [22] while other research groups using a direct measurement system report results up to 700°C [20].

Various etching techniques were investigated for the fabrication of 3D AlN devices. Wet etching was deemed an infeasible technique for fabricating AlN devices because the etch rate is highly dependent on the crystal quality of the material. Since it is desirable to use high quality material for AlN devices, wet etching is not the optimal technique. Dry etching using an inductively coupled plasma (ICP) system with a BCl_3/Cl_2 gas mixture was investigated because of its capability for etching high quality AlN. A thorough etch characterization was conducted to determine how the etch mechanism is effected by adjusting the system parameters. The optimal parameters chosen for etching AlN are 100 W RIE power, 400 W ICP power, 20 mTorr pressure, 15 sccm BCl_3, and 15 sccm Cl_2. The etch rates of sputtered and MOVPE-AlN on GaN are roughly 80 and 66 nm/min, respectively.

Mesa structures were fabricated to enhance the piezoelectric response of AlN by eliminating non-normal electric field lines which give rise to the transverse piezoelectric coefficient (d_{31}). A top down fabrication technique was used to make mesa structures out of high quality sputtered and MOVPE-grown AlN films using the dry etching technique described in chapter 4. Piezoelectric measurements indicate that the piezoelectric response is dependent on the size of the mesa structures and the material used for the top and bottom electrodes. The Pt/AlN/Pt structure exhibits the largest piezoelectric response and the Al/AlN/Al structure exhibits the lowest. The piezoelectric response of the mesas is clearly dependent on the size of the mesas as well, with large mesas exhibiting the largest response.

A new mask was designed to allow mapping of the piezoelectric response of same-sized mesa structures over an entire sample. To determine the differences in the piezoelectric response of mesas as compared to films, an experiment was performed to measure the d_{33} over an entire AlN film prior to mesa fabrication. Then the film was etched into mesas and the d_{33} of the mesas was measured. The piezoelectric response varied across the film due to changes in crystal quality and thickness in the sputtered film. The piezoelectric response increased in over 50% of the contacts that were etched into mesa structures with the piezoelectric coefficient nearly doubling in some cases. The variance in the piezoelectric response of the mesas can also be attributed to non-uniform crystal quality and thickness variation of sputtered films. Current work is being performed to quantify the increase of the piezoelectric response of AlN mesas.

The goal of this work was to build upon the high temperature piezoelectric characterization of AlN films and establish a method for performing in-situ high temperature measurements of 3D AlN devices. Understanding the effects of high temperatures and harsh environments is important for AlN MEMS applications. In this work, oxidation trends and the in-situ piezoelectric response of AlN were measured. In the future, it will be important to establish an in-situ measurement technique that will allow for measurements to be conducted above 300°C for sputtered AlN films and mesas. Ultimately, this work will lead to high temperature piezoelectric measurements of 3D AlN structures.

BIBLIOGRAPHY

[1] W. S. Trimmer (ed.), Micromechanics and MEMS Classic and Seminal Papers to 1990, IEEE Press, New York, 1997

[2] J. Bryzek, K. Petersen, and W. McCulley, "Micromachines on the March," IEEE Spectrum, 31(5):20 (1994)

[3] K. Petersen, "Silicon as a Mechanical Material," IEEE Proc. 70:420 (1982)

[4] G. Cibuzar and S. Campbell (ed.), The Science and Engineering of Microelectronic Fabrication , Oxford University Press, New York (2001)

[5] B. A. Auld, Acoustic Fields and Waves in Solids, Wiley-Interscience, New York, 1973

[6] W. G. Cady, Piezoelectricity, McGraw-Hill, New York, 1964

[7] The Piezoelectric Effect < www.aurelienr.com/electronique/piezo/piezo.pdf>

[8] S. Trolier-McKinstry & P. Muralt, Journal of Electroceramics, 12 (2004) 7-17

[9] J. P. Kar, G. Bose, Tuli, Surface and Coatings Technology, 198 (2005) 64-67

[10] Aluminum Nitride Ultraviolet Light-emitting Diode with the Shortest Emission Wavelength <www.ntt.co.jp/RD/OFIS/active/2007pdfe/pdf/h_ct07_e.pdf>

[11] H. L. Kao, P. J. Shih and Chun-His Lai, Japanese Journal of Applied Physics, 38 (1999) 1526-1529

[12] N. Kumar, K. Pourrezaei, J. J. De Maria and B. Singh, Materials Research Society Symposium Proceedings, 68 (1986) 357-363

[13] B. Mednikarov, G. Spasov, Tz. Babeva, Journal of Optoelectronics and Advanced Materials, 7, 3 (2005) 1421-1427

[14] Kuo-Sheng Kao, Chung-Jen Chung, Ying-Chung Chen, Tien-Fan Ou, Tai-Kang Shing, 2004 IEEE Internations Ultrasonics, Ferroelectrics, and Frequency Control Joint 50th Anniversary Conference

[15] Marc-Alexandre Dubois, Paul Muralt, Journal of Applied Physics, 89, 11 (2001)

[16] J. Harman, A. Kabulski, V. R. Pagán, P. Famouri, K. R. Kasarla, L. E. Rodak, J. Peter Hensel, D. Korakakis, Journal of Vacuum Science Technology B, 26, 4 (2008) 1417-1419

[17] N. Fujimoto, T. Kitano, G. Narita, N. Okada, K. Balakrishnan, M. Iwaya, S. Kamiyama, H. Amano, I. Akasaki, K. Shimono, T. Noro, T. Takagi, and A. Bandoh, Physica Status Solidi (c) 3, 6 (2005) 1617-1619

[18] R. C. Turner, P. A. Fuierer, R. E. Newnham, T. R. Shrout, Applied Acoustics, 41 (1994) 299-32

[19] C. Miclea, C. Tanasoiu, L. Amarande, C. F. Miclea, C. Plavitu, M. Cioangher, L. Trupina, C. T. Miclea, C. David, Romanian Journal of Information Science and Technology, 10, 3 (2004) 243-250

[20] Kazushi Kishi, Yasunobu Ooishi, Hiroaki Noma, Eizo Ushijima, Naohiro Ueno, Morito Akiyama, Tatsuo Tabaru, Journal of European Ceramic Society, 26 (2006) 3425-3430

[21] F. Engelmark, G. Fucntes, I. V. Katardjiev, A. Harsta, U. Smith, and S. Berg, Journal of Vacuum Science Technology A, 18, 4 (2000) 1609-1612

[22] Morito Akiyama, Toishihiro Kamohara, Kazuhiko Kano, Akihiko Teshigahara, Nobuaki Kawahara, Applied Physics Letters, 93, 021903 (2008)

[23] D. Bloor, R. J. Brook, M. C. Flemings, S. Mahajan, "The Encyclopedia of Advanced Materials Vol. 1". (Pergamon Press, Cambridge, 1994) p. 86

[24] Y. Geng, G. Norton, Journal of Materials Research, 14 (1999) 2708.

[25] A. Bellosi, E. Landi, A. Tampieri, *ibid*. 8 (1993) 565

[26] E. W. Osborne, M. G. Norton, Journal of Materials Science, 33 (1998) 3859

[27] A. L. Brown, M. G. Norton, Journal of Materials Science Letters, 17 (1998) 1519

[28] J. W. Lee, I. Radu, M. Alexe, Journal of Materials Science: Materials in Electronics, 13 (2002) 131-137

[29] F. L. Riley, Advanced Ceramic Materials (1996)

[30] Y. Watanabe, N. Kitazawa, Y. Nakamura, C. Li, T. Sekino, K. Niihara, Journal of Vacuum Science Technology A, 18 (2000) 1567

[31] L. Vergara, J. Olivares, E. Iborra, M. Clement, A. Sanz-Hervás, J. Sangrador Thin Solid Films, 515 (2006) 1814-1818

[32] Kazuhiko Kano, Kazuki Arakawa, Yukihiro Takeuchi, Morito Akiyama, Naohiro Ueno, Nobuaki Kawahara, Sensors and Actuators A, 130-131 (2006) 397-402

[33] Kazushi Kishi, Yasunobu Ooishi, Hiroaki Noma, Eizo Ushijima, Naohiro Ueno, Morito Akiyama, Tatsuo Tabaru, Journal of European Ceramic Society, 26 (2006) 3425-3430

[34] Y. Watanabe, Y. Hara, T. Tokuda, N. Kitzawa, and Y. Nakamura, Surface Engineering, 16, 13 (2000)

[35] V. Fuflyigin, E. Salley, A. Osinsky, P. Norris, Applied Physics Letters, 77, 19 (2006) 3075-3077

[36] Everett E. Crisman, John S. Derov, Alvin J. Drehman, and Otto J. Gregory, Electrochemical and Solid State Letters, 8, 3 (2005) H31-H32

[37] W. M. Yim, R. J. Paff, Journal of Applied Physics, 45, 3 (1974) 1456-1457

[38] K. M. Taylor, C. Lenie, Journal of the Electrochemical Society, 107, 308 (1960)

[39] G. Long, L. M. Fuster, Journal of the American Ceramic Society, 41, 53 (1959)

[40] N. J. Barrett, J. D. Grange, B. J. Sealy, K. G. Stephens, Journal of Applied Physics, 57, 5470 (1985)

[41] C. R. Aita, C. J. Gawlak, Journal of Vacuum Science Technology A, 1, 403 (1983)

[42] G. R. Kline, K. M. Lakin, Applied Physics Letters, 43, 750 (1983)

[43] J. R. Mileham, S. J. Pearton, C. R. Abernathy, J. D. MacKenzie, R. J. Shul, S. P. Kilcoyne, Applied Physics Letters, 67, 8 (1995) 1119-1121

[44] Leo J. Schowalter, Juan C Rojo, Nikolai Yakolev, Yuriy Shusterman, Katherine Dovidenko, Rungjun Wang, Ishwara Bhat, Glen A Slack, MRS Internet Journal of Nitride Semiconductor Research, 5S1, W6.7 (2000)

[45] D. Zhuang, J. H. Edgar, Lianghong Liu, B. Liu, L. Walker, MRS Internet Journal of Nitride Semiconductor Research, 7, 4 (2002)

[46] D. Zhuang, J. H. Edgar, Material Science and Engineering, R 48, 1 (2005)

[47] I. Cimalla, Ch. Foerster, V. Cimalla, V. Lebedev, D. Cengher, and O. Ambacher. Physica Status Solidi © 3, 6, (2006) 1767-1770

[48] R. J. Shul, L. Zhang, C. G. Willison, J. Han, S. J. Pearton, J. Hong, C. R. Abernathy, L. F. Lester. MRS Internet Journal of Nitride Semiconductor Research, 4, 1 (1999)

[49] Richard S. Muller and Theodore I. Kamins (ed.). John Wiley & Sons (Asia) Pte. Ltd., Signapore (2003)

[50] R. J. Shul, G. A. Vawter, C. G. Willison, M. M. Bridges, J. W. Lee, S. J. Pearton, C. R. Abernathy. Solid State Electronics, 42, 12 (1998) 2259-2267

[51] R. J. Shul, C. G. Willison, M. M. Bridges, J. Han, J. W. Lee, S. J. Pearton, C. R. Abernathy, J. D. MacKenzie, S. M. Donovan. Solid State Electronics, 42, 12 (1998) 2269-2276

[52] F. A. Khan, L. Zhou, V. Kumar, I. Adesida, R. Okojie. Materials Science and Engineering, B95 (2002) 51-54

APPENDIX A – CONTACT MASK DESIGN

The large standard deviation in the original measured displacement of the AlN mesa structures was partly a result of the small sampling of each contact size on every sample. The number of contacts of the same size was limited and they were in remote proximity making it difficult to determine if varying results were the cause of areas of different film quality or simply an erroneous measurement. Due to the less uniform crystal orientation of sputtered AlN films, it is important to know how the piezoelectric response varies across a sample.

A mask was designed using the L-Edit mask designing software grouping same-sized contacts close to one another to allow for an increased number of measurable contacts on each film. The larger sampling improves the accuracy of the mean value used to distinguish the piezoelectric response. The even distribution of same-sized contacts in the mask design allows for surface mapping of d_{33} trends over an entire sample. Circular contacts of 100 μm, 200 μm, 300 μm, and 400 μm radius were of particular interest for comparison to measurements of the same-sized mesas fabricated using the previous mask. To further investigate the piezoelectric response dependence on the contact size, contacts of 500 μm, 600 μm, 700 μm, 800 μm and 1 mm radius were also designed on the mask. The new mask design makes surface mapping easier with labels distinguishing each contact. The response measured from each contact is more easily linked to a specific area on the sample.

One particular area of interest in the study of AlN films and mesas is the effect of contact size on the measured piezoelectric response. The design of the previous mask made it difficult to determine whether the difference in response from one sized contact to the next was due to the size difference or the location of the contact on the film. The new mask is designed for mapping the piezoelectric response of different contact sizes in roughly the same area of the film. Figure 32 shows a matrix of 300 µm radius contacts within a matrix of 400 µm radius contacts. Different sections of the mask employ the same design with 200 µm and 100 µm radius contact matrices within the 400 µm matrix.

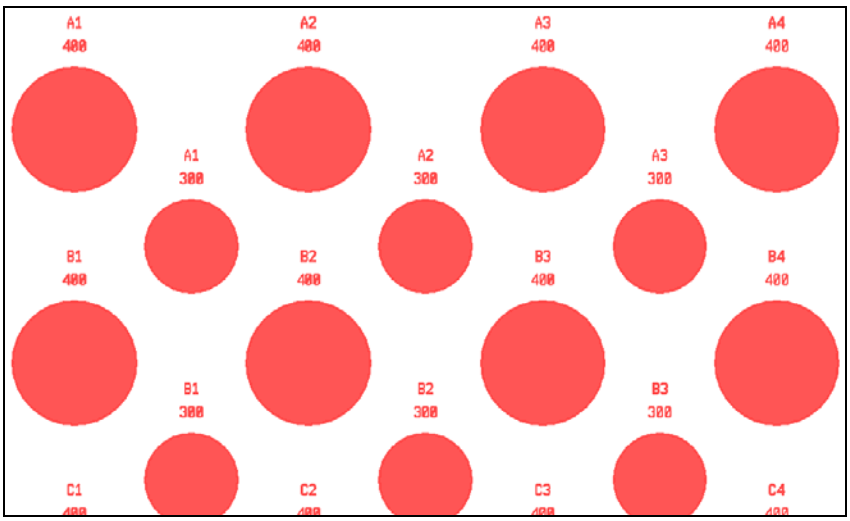

Figure 32 – 400 µm and 300 µm radius contacts intermixed in mask design

The new mask was also designed to address the issue of whether the radius of the mesas or the radius of the contacts has a larger impact on the piezoelectric response. To determine which effect is more prominent, the new mask design makes it possible to fabricate mesas with a large radius with smaller sized contacts on top. Figure 33 shows a portion of the mask layout designed to fabricate large mesas with smaller contacts. Two

other sections of the new mask have contacts of 100 μm and 200 μm radius with alignment marks making it possible to combine any combination of the mesa and contact size.

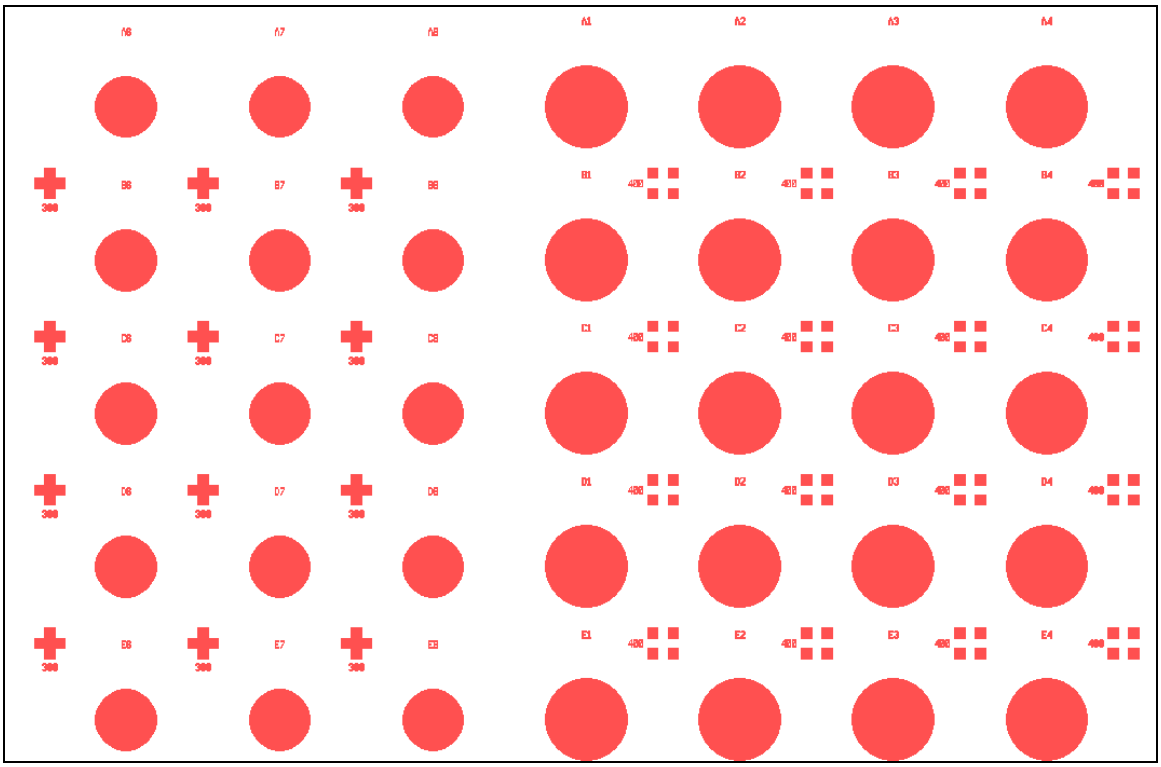

Figure 33 – Realignment capabilities made possible by the mask